CR-152038

INVESTIGATION OF THE EFFECTS OF A MOVING ACOUSTIC MEDIUM ON JET NOISE MEASUREMENTS

by

John E. Cole, III
Douglas W. Palmer

December 1976

(NASA-CR-152038) INVESTIGATION OF THE EFFECTS OF A MOVING ACOUSTIC MEDIUM ON JET NOISE MEASUREMENTS (Tufts Univ.) 91 p HC A05/MF A01 CSCL 20A

N77-29921

Unclas
G3/71 44014

Prepared under NASA-Ames University Consortium
Interchange NCA2-OR785-601 by
TUFTS UNIVERSITY
Medford, MA

for

NATIONAL AERONAUTICS AND SPACE ADMINISTRATION
Ames Research Center
Moffett Field, California

SUMMARY

The noise from an unheated sonic jet in the presence of an external flow is measured in a free-jet wind tunnel using microphones located both inside and outside of the flow. Comparison of the data is made with the results of other studies which have measured jet noise in the presence of flow with either in-wind or out-of-wind microphones. The results are also compared with existing theoretical predictions of the source strength for jet noise in the presence of flow and of the effects of sound propagation through a shear layer.

TABLE OF CONTENTS

1.0 INTRODUCTION

The characteristics of jet mixing noise in the presence of an external flow determine a large portion of the noise generated by an aircraft in flight. Certification requirements on aircraft noise in flight have provided the motivation for establishing adequate prediction methods for many aircraft noise sources including jet mixing noise.

While the noise from existing aircraft configurations can be measured during flight tests, it is useful to use a flight simulation technique to assess the noise from modified or new configurations. There are several methods and facilities which have been used to simulate the effects of flight on jet noise. Several of these methods are described in reference 1. Perhaps the most commonly used type of facility for this purpose is the wind tunnel. Measurements of jet noise in the presence of flow have previously been made in conventional wind tunnels such as the 12-by 24 meter (40-by 80 feet) facility of NASA Ames Research Center (refs. 2,3) and the 7.3 meter (24 feet) facility of the Royal Aircraft Establishment (ref. 4) as well as in free-jet wind tunnels such as the facilities of United Technologies Research Laboratories, (refs. 1,5) and the Lockheed-Georgia Company (ref. 6).

There are several experimental difficulties associated with assessing the characteristics of jet noise in the presence of flow using either type of wind tunnel facility.

In a conventional wind tunnel which has not been specifically designed or modified for acoustic measurements, there is often a large amount of background noise from the drive system when the wind tunnel is operating. Microphones placed in the wind tunnel flow are therefore subject not only to significant wind noise generated by the flow over the microphone, but also to the background noise. In addition, conventional wind tunnels are generally highly reverberant making a free-field simulation even more difficult. The studies reported in references 2 and 3 use full-scale jet engines as noise sources. Microphones placed near to the source in order to minimize the large reverberant field near the walls of the wind tunnel are therefore in the near field over frequency ranges of interest. While some of these difficulties are not present in the free-jet facilities, other problem areas exist. The free-jet wind tunnel may be designed to be reasonably quiet by isolating the fan and drive system and by acoustically treating the chamber in which the free-jet is established. Problems associated with background noise and the reverberant field are therefore minimized. In order to obtain data in the far-field of a source and to eliminate wind noise, the usual procedure is to place the microphones outside of the wind tunnel flow. This procedure introduces a difficulty in interpretation of data recorded by the microphones located out of the wind. Sound propagating from a source located inside the flow of the wind tunnel is refracted and scattered by the turbulent shear layer of the flow. The interpretation of noise data taken in this manner relies on corrections supplied by various theoretical analyses and models of sound propagation through the shear layer.

The motivation of the present study is to measure the mixing noise from an unheated jet in the presence of flow with microphones located in the flow under reasonably anechoic conditions. The experiment is designed so that the measurements are made in the far-field of the source over most of the frequency range of interest. For this purpose a free-jet wind tunnel is used. Another aspect of this experiment is the use of additional microphones located outside the wind tunnel flow. Data obtained from the simultaneous measurements of jet noise by microphones located both inside and outside the flow are used to assess the prediction of a theoretical model of sound propagation through a shear layer.

In order to accomplish the goals of this study, certain compromises in operating conditions and geometry are necessary. For the dimensions of the wind tunnel used, acoustic and geometric far-field conditions are approximated for the microphones located within the flow by using a model jet with an exit diameter of .013 (0.5 in) meter. Under conditions of high flow speed, it is found that the wind noise in the microphone overwhelms the jet noise from this size model jet. As a result, the maximum flow speed used in this study is 42.7 m/s (140 f/s).

2.0 EXPERIMENTAL APPARATUS

The test facility used for this study is the free-jet wind tunnel of Bolt, Beranek and Newman, Inc. This facility consists of an acoustically treated chamber in which a free-jet flow is established. The dimensions of the chamber are 7 m (23 ft) by 13.4 m (44 ft) by 6.1 m (20 ft) in height giving a total volume of 572 m^3 (20240 ft^3). The walls, floor, and ceiling are covered with 5.08 cm (2 in) thick open cell foam. The room is essentially anechoic for frequencies above 160 Hz (ref. 7).

The wind tunnel operates in a suction mode. As indicated in figure 1 outside air enters the room through a convergent nozzle with a contraction ratio of 15.5. The nozzle used for this study is rectangular in cross-section with exit dimensions of 0.711 m (28 in) by 1.02 m (40 in). The centerline of the tunnel nozzle is 2.44 m (8 ft) above the floor. A stagnation plate collector at the opposite end of the chamber returns the air to the fan. The fan is powered by a 448 kw (600 Hp) diesel engine.

The aerodynamic performance of the wind tunnel is discussed in reference 7. For a slightly different nozzle, the mean velocity at the exit plane is reported to be uniform within .25% for flow velocities greater than 27.4 m/s (90 f/s). The overall turbulence level in the potential core of the wind tunnel flow is reported to be .23%. The turbulence spectrum for three wind speeds is also found in reference 7.

An unheated model jet is located within the potential core of the tunnel flow. As shown in figure 2 the exit plane of the model jet extends 46 cm (18 in) beyond the end of the wind tunnel nozzle. This location allows microphone positions to extend to angles up to 115° from the jet axis. The model jet is centered vertically with respect to the wind tunnel nozzle, but it is located 20. cm (8 in) to one side of the centerline of the wind tunnel. This asymmetric positioning allows microphones to be placed in the wind tunnel flow at a minimum distance of one wavelength away from the model jet for frequencies greater than 600 Hz. The exit diameter of the model jet is 1.3 cm (0.5 in). The nozzle has an overall length of 6.35 cm (2.50 in) with an inlet diameter of 5.08 cm (2 in) giving a contraction ratio of 16 :1 (see fig. 3).

The source of compressed air for the model jet is an industrial air-compressor. The high pressure supply air is throttled down to 1.0×10^5 pascals (15 psig) by means of a 1.6 cm (0.62 in) diameter orifice plate. Several stages of muffling and noise surpression are added between the orifice plate and the nozzle of the model jet (see fig. 4). After the orifice plate the supply air flows through two inline mufflers. The air then enters a .34 m^3 (12 ft^3) plenum and leaves through 6.1 m (20 ft) of 20. cm (8 in) metal ducting which brings it to a large muffler of volume 0.2 m^3 (7.2 ft^3). A 3.0 m (10 ft) length of 5.1 cm (2 in) diameter copper tubing extends from the muffler to the nozzle. The last 102. cm (40 in) of tubing is straight. In this last section turbulence remaining in the supply air is further suppressed. As indicated in figure 3, within this straight section are three fine mesh copper screens to break up large eddies and a 15. cm (6 in) length of .64 cm (1/4 in) diameter plastic tubes which are packed in a bundle to serve as flow straighteners. All diameter changes in the final stage of the air supply are made to be reasonably gradual and smooth.

The flow speeds of both the wind tunnel and the model jet are determined from total pressure measurements. The total pressure of the wind tunnel flow is measured by a pitot tube positioned 10. cm (4 in) above the lower wall of the wind tunnel nozzle as indicated in figure 2. This pitot tube is connected to a water manometer. The total pressure of the model jet is measured by a pitot tube centered in the 5.1 cm (2 in) diameter tubing of the final air supply (see fig. 4). This pitot tube is connected to a mercury manometer.

Acoustic measurements are made using .64 cm (0.25 in) Brüel and Kjaer model 4135 microphones with model UA 0385 nose cones. Each microphone is attached to a cathode follower and a preamplifier. The microphone signals are input to a Brüel and Kjaer signal conditioner to equalize sensitivities. An Ithaco amplifier further amplifies the signal. A switch box allows the signal to be sent to any of the following three instruments: Brüel and Kjaer Precision Sound Level Meter; magnetic tape recorder; General Radio 1921 Real Time Spectrum Analyzer. A schematic of the instrumentation is shown in figure 5. A copy of the one-third octave band spectral analysis is obtained either as a plot from an x-y plotter or a teletype and paper tape output.

During the test procedure two microphones are used simultaneously. Both are located along the same optical ray originating at the center of the model jet nozzle. When the wind tunnel is operating one microphone (the 'in-wind' microphone) is located within the potential core of the flow while the other (the 'out-of-wind' microphone) is located outside of the wind tunnel flow. During the testing sequence, both microphones are positioned at angles from 20° to 115° relative to the jet axis. The specific microphone positions are given in Table I and figure 2. Note that the smallest angle of the 'out-of-wind' microphone is 25° when the angle of the 'in-wind' microphone is 20°. The closest distance of the in-wind microphone from the model jet is 58.4 cm (23 in). This occurs at an angle of 90° relative to the jet axis. At this distance the value of kr (acoustic wave number times microphone distance) is greater than 2π for all frequencies greater than 600 Hz. This indicates acceptable acoustic far-field conditions over the frequency range of interest for jet noise. This distance is also equal to 46 diameters of the model jet which indicates that the microphones are also in the geometric far-field of the jet noise source.

Position changes of the in-wind microphone during testing are facilitated by mounting it on a horizontal straight track 1.52 m (5.0 ft) above the floor. The track and its supporting members are positioned below the wind tunnel flow. A 0.91 m

Table I. Positions of "In-Wind" and "Out-of-Wind" Microphones.

ANGLE ψ (DEGREES)	DISTANCE (meters)	
	IN-WIND Microphone	OUT-OF-WIND Microphone
20	1.37	---
25	---	5.77
30	1.04	4.88
40	0.832	3.79
50	0.717	3.18
60	0.648	2.81
70	0.603	2.60
80	0.589	2.48
90	0.584	2.44
100	0.597	2.48
110	0.622	2.60
115	0.654	2.69

(3 ft) length of 1.9 cm (0.75 in) diameter steel rod is positioned vertically on the track. The in-wind microphone is firmly attached to the top of the rod and oriented directly upstream. As shown in figure 6, the rod and microphone are prevented from moving in the wind by supporting the rod with four thin stainless steel wires. The entire structure is wrapped with 0.64 cm (.25 in) foam to minimize possible reflections of the jet noise.

The out-of-wind microphone is located in the quiescent air of the room beyond the turbulent shear layer of the wind flow at a sideline distance of 2.44m(8.0 ft). It is held in a microphone stand at the top of a 2.44 m (8 ft) vertical pole. The assembly is manually moved from one position to the next during the testing sequence. Although not exposed to the flow, the out-of-wind microphones are also fitted with model UA 0385 nose cones and oriented to point in the same upstream direction as the in-wind microphones. This procedure is adopted in order to maintain the same response characteristics at high frequencies as the in-wind microphones.

3.0 THEORETICAL CONSIDERATIONS

3.1 Source Strength Alterations

There are several reasons for expecting differences in the characteristics of static jet noise and jet noise in the presence of flow. Differences are to be expected in the nature of the turbulent flow field of the jet itself. For the same exit velocity of the jet, the presence of a co-flowing medium is found to decrease the mean velocity shear rate, alter the turbulence level, and extend the potential core region of the jet (ref. 13). Such differences would be expected to alter the source strength of the jet noise. On the basis of dimensional arguments, Ffowcs Williams (ref. 8) gives the following dependence of the source strength for a cold jet in the presence of a flow:

$$S_j \; \alpha \; (V_j - V_o)^7 \, V_j \tag{1}$$

where V_j is the jet exit velocity and V_o is the flow velocity. A modification of this result accounting for the extension of the potential core region of the jet is given by Cocking and Bryce (ref. 4). This result is

$$S_j \; \alpha \; (V_j - V_o)^7 \, V_j \, \frac{(V_j + V_o)}{(V_j + .3V_o)} \tag{2}$$

More recently Sarohia and Massier (ref. 9) have suggested another aspect of the flow which could effect the source strength. This is the interaction of the boundary layer of the flow over the surface of the jet nozzle with the turbulent jet flow. An analysis of the effects of this interaction suggests a rescaling of the source strength as follows:

$$S_j \propto \frac{V_j^{9}}{(V_j - V_o)} \tag{3}$$

3.2 Coordinate Systems for Moving Sources

The origin of jet noise is usually conceived of as fluctuating turbulent eddies which are in motion with velocity V_c relative to the exit of the jet nozzle. Theoretical models of jet noise such as those of Ribner, (ref. 10), Ffowcs Williams (ref. 8), Mani (ref. 11) and Tester and Morfey (ref. 12) are used to calculate the acoustic field based on a source moving with constant speed. There are two conventional ways of expressing the acoustic pressure field of a moving source. The acoustic pressure at the position of an observer may be expressed relative to the position of the source at the time that the acoustic "signal" is either emitted or received. When the source of sound is convecting turbulence, it is customary to use the position of the source at the time the signal is emitted. This is reasonable since the turbulent source may have lost its identity by the time the signal is received. When the observer is in the geometric far-field of the jet noise, the source position is usually taken to be the exit of the jet nozzle.

When jet noise is emitted by an aircraft in flight, there are again two obvious choices for the source position (see fig. 7). The jet noise (either measured or calculated) at an observer may be referred to the aircraft position at the time of either signal emission (emission coordinates) or signal reception (reception coordinates). It is customary to report data from aircraft flyover tests in terms of the emission coordinates (R, θ). This is particularly useful for incorporating the effects of atmospheric attenuation since R is the actual distance through which the sound propagates from source to observer.

The effects of flight on jet noise may be simulated using wind tunnels. The noise received by microphones located in the wind is most conveniently reported in terms of the reception coordinates. Under geometrical far-field conditions the position of the in-wind microphones from the jet nozzle (r,ψ) give identically the coordinates of the source at the time of signal reception. Jet noise data in terms of reception coordinates in a wind tunnel simulation may be "corrected" to give the equivalent data in terms of emission coordinates. The two coordinate systems are related through the geometry of figure 7 as follows (ref. 10):

$$R = r \left(\frac{S - M_o \cos\psi}{1 - M_o^2}\right) \tag{4}$$

$$\cos\theta = \frac{\cos\psi - M_o S}{S - M_o \cos\psi} \tag{5}$$

where

$$S = \sqrt{1 - M_o^2 \sin^2\psi} \tag{6}$$

For data reported at constant distance from the source, these relationships imply a change in both angle and noise level.

3.3 Doppler Shift

One of the basic characteristics of the sound field of a moving source is the Doppler shift in frequency. When a source moves with constant velocity through an acoustic medium at rest, the frequency shift is given in reference 13 as

$$\frac{f(\theta)}{f_o} = \frac{1}{1 - M\cos\theta} \tag{7}$$

where f_o is the frequency of the source, θ is the emission angle, and M is the Mach number of the source relative to the observer. In the case of the models of jet noise from an aircraft in flight,

$$M = M_c - M_o \tag{8}$$

where M_c is the Mach number of the convecting sources relative to the jet nozzle and M_o is the Mach number of the aircraft.

The form of the Doppler shift from a moving source in terms of the reception coordinates is given in reference 14 to be

$$\frac{f(\psi)}{f_o} = \frac{(1-M_o^2)S}{(1+M_cM_o-M_o^2)S-M_c\cos\psi} \tag{9}$$

where S is defined in equation (6). If in fact jet noise is well modeled by sources moving with constant velocity (careful measurements of static jet noise cast some doubt on this modeling (ref. 15)), then the Doppler shift relationships for emission and reception coordinates are given by equations (7) and (9) respectively. The frequency spectrum of jet noise measured in a wind tunnel simulation using reception coordinates must therefore be "corrected" to obtain the corresponding frequency spectrum from an aircraft in flight, using emission coordinates. The relationship between $f(\theta)$ and $f(\psi)$ is obtained by combining equations (5), (7), and (9) with the result

$$f(\theta) = f(\psi)\,\frac{(S-M_o\cos\psi)}{(1-M_o^{\,2})S} \qquad (10)$$

When the approximation is made that $M_o^{\,2} \ll 1$, the relationship reported in reference 4 is obtained

$$f(\theta) \cong f(\psi)\,(1-M_o\cos\psi) \qquad (11)$$

3.4 Shear Layer Corrections

In a simulation of the effects of flight using a free-jet wind tunnel, the jet noise reaching the out-of-wind microphones propagates through the turbulent shear layer of the wind tunnel flow. The region of the shear layer which bounds the potential core of the wind tunnel flow grows as the flow proceeds downstream. The effects of this shear layer on acoustic propagation are to refract, scatter, and perhaps reflect the jet noise.

Various aspects and models of sound propagation through such a shear layer have been treated analytically. Scattering of sound by the turbulence has been treated theoretically by Rudd (ref. 16) among others. Measurements of the effects of scattering by turbulence in the shear layer of a free-jet wind tunnel are presented by Candel, et al. (ref. 17). This latter study reports a significant effect of forward scattering by the turbulence on sound propagating at angles of approximately ninety degrees to the flow direction.

Sound propagation through a region of mean velocity shear has been investigated theoretically by Amiet (ref. 18), Mani (ref. 11), Tester and Burrin (ref. 19), Tester and Morfey (ref. 12), and others. One of the simplest models is that of Amiet. In this model an arbitrary point source is located in a uniform flow. The flow is separated from a semi-infinite region of no flow by a plane shear layer of zero thickness. Combining the boundary conditions appropriate to the interface with geometrical acoustics, Amiet determines explicit relationships for the acoustic pressure in the region of no flow. The result of the analysis is a prediction of the acoustic field which would be present in the uniform flow if the shear layer were absent. Mani has investigated the effects of source type on sound propagation through a cylindrical shear layer of zero thickness. A solution using geometrical acoustics for sound propagation through thick shear layers with assumed velocity profiles has been calculated by Shubert. Models based on the Lilley equation have been calculated by Tester and Burrin and Tester and Morfey. Although these latter approaches can account for more of the detailed structure of the flow, the results are less easy to generalize or to use for an arbitrary application.

4.0 DATA QUALITY

As a means of assessing the quality of the jet noise data obtained during this experiment, comparison is made with several other static jet noise predictions and studies. The data used in these comparisons are measured under the conditions of zero wind tunnel velocity. The experimental uncertainty for the level of the overall sound pressures reported for the present study is estimated to be ±.5 dB.

The Society of Automotive Engineers in a proposed revision of Aerospace Information Report 876 (ref. 21) provides a method for the prediction of static jet noise. The information required to use this method is the jet exit velocity, the weight density of the fully expanded jet, the cross-sectional area of the jet, and the distance of the observer from the jet. The procedure outlined in reference 21 yields a one-third octave band spectrum plotted against the logarithm of the Strouhal number (i.e., $\log_{10} (\frac{fD}{V_j})$, where f is the frequency, D is the exit diameter of the jet, and V_j is the exit speed of the jet). Figure 8 shows the measured jet data at 60° relative to the jet axis along with the predicted spectrum. The two curves agree for frequencies below a Strouhal number of about .3. At higher frequencies the measured sound pressure levels are lower than those predicted. The predicted overall sound pressure level is 3 dB greater than the measured level. These results indicate that there may be some contamination in the high frequency range of the jet noise measured in this study. The procedure of reference 21 also predicts the directivity of the overall sound pressure level. The measured directivity of the overall sound pressure level in this study is shown in figure 9 along with the predicted directivity. The shapes of the two curves are similar with differences in level ranging from .4 dB to a maximum of 3.0 dB. The measured overall sound pressure levels are consistently less than those predicted, perhaps due to a reduction in the high frequency components as indicated above.

A different prediction method for static jet noise is described by Stone (ref. 22). Figure 10 shows the predicted and measured one-third octave band spectrum at an angle of 30° relative to the jet exit direction. At the lower frequencies (i.e. Strouhal numbers less than .4), the measured spectrum agrees very well with the predicted spectrum. At the higher frequencies, the measured levels drop below the predicted values. The predicted overall sound pressure level at an angle of 90° is 93 dB. The measured overall sound pressure level at 90° is 89 dB, a difference of 4 dB.

A thorough and careful study of subsonic jet noise from an unheated jet is reported by Ahuja and Bushell (ref. 15). One presentation of the results is a directivity of the mean-square pressure in one-third octave bands. The particular one-third octave bands are functions of convection Mach number and angle. They are chosen to correspond with specific values of the Doppler shifted Strouhal number. This Strouhal number is given by $(\frac{fD}{V_j})(1-M_c\cos\theta)$ where M_c is the convection Mach number. The values chosen for the Doppler shifted

Stouhal number are .03, .10, .30, and 1.0.

The data of Ahuja, for a jet with Mach number of 0.90, are presented on figure 11. Also shown is the sonic jet data of the present study for the same Doppler shifted Strouhal numbers. The dependence of the jet-noise data on measurement distance (r) and jet nozzle exit area (A_j) is removed from both sets of data by adding a term of $-10 \log_{10}(\frac{A_j}{r^2})$ to the measured sound pressure levels. For the lower values of the corrected Strouhal number, (i.e., .03, .10, .30), the two sets of data are of similar shape and slope. The sonic jet data tend to be approximately four dB higher for each of these curves than the data from the subsonic jet of Ahuja. It is suspected that this difference in sound pressure levels is due to the difference in the jet velocities used in reference 15 and in the present study. The method of reference 21 predicts that the difference in sound pressure levels from data of Mach numbers .90 and 1.0 is 4.2 dB. At the value of the Doppler shifted Strouhal number of 1.0, the data from this study differ markedly from that of Ahuja. This again suggests that the higher frequency components of our measured jet noise may have been contaminated in some manner.

Jet noise measurements are made simultaneously by two microphones located at different distances (r_1 for the in-wind microphone and r_2 for the out-of-wind microphone) along an optical ray extending from the exit of the net nozzle. As described above, both microphones are located far enough from the nozzle to be considered in the acoustic far-field of the jet. In the acoustic far-field the acoustic pressure should vary inversely with the distance from the source. For the static jet noise data the difference in sound pressure levels measured by the in-wind microphone and the out-of-wind microphone should be given by 20 $\log_{10}(\frac{r_1}{r_2})$. It is found that this is not observed over the entire one-third octave band spectrum. The difference in the sound pressure levels measured by the two microphones in the lower frequency components (below approximately 10 KHz) is consistent with the acoustic far-field dependence. Deviation from this dependence is, however, found in the higher frequency components where an increased difference in levels is measured. This suggests that the sound pressure levels of the higher frequency components are not entirely due to direct radiation of the jet noise source but may also contain some reflected noise or other contamination.

The static jet noise data in this study tend to deviate from previously established data and from acoustic far-field dependence for Strouhal numbers greater than approximately .32. For this experiment, a Strouhal number of .32 indicates a frequency of 8600 Hz with an associated wavelength of 4 cm (1.6 in). Such a wavelength is comparable with the dimensions of the structural supports for the in-wind microphone. It is therefore suspected that significant acoustic scattering from these supports contaminates the data at the high frequencies.

These comparisons indicate that the low frequency portion of the jet noise data from this study is representative of pure jet mixing noise. The higher frequency components, however, appear to be contaminated owing to reflections from the microphone support structure.

5.0 RESULTS AND DISCUSSION

5.1 Data Reduction Procedure

There are several test conditions under which data are taken. The wind noise on the microphones is measured at wind speeds of 30.5 m/s (100 f/s) and 42.7 m/s (140 f/s) and sonic jet noise is measured with no wind tunnel flow. Measurements are also made of sonic jet noise in the presence of flow at wind tunnel speeds of 30.5 m/s and 42.7 m/s. For each test condition the acoustic pressure is measured at eleven angular positions. At each angle there are two microphone locations as shown on figure 2. Each of the microphones is connected in turn to the real time analyzer. The output from the real time analyzer is the sound pressure level at each of 27 one-third octave bands. The one-third octave band center frequencies range from 160 Hz to 63 KHz.

The frequency response of the B & K model 4135 microphones is flat to approximately 4000 Hz. However, at higher frequencies the microphone's actuator response decreases continuously. Both the in-wind and out-of-wind microphones are fitted with B & K model UA 0385 nose cones. The pressure response of the microphone with the nose cone is a function of both the frequency and the angle of incidence. The corrections for the free-field frequency response of the microphone with the nose cones is provided by Brüel and Kjaer (ref. 23) in angular increments of 30 degrees of incidence. The free-field pressure response of the microphones is obtained by adding the actuator response (ref. 23) to the nose cone corrections. Any difference of the free-field pressure response determined in this manner from the flat response sensitivity is called a free-field correction. All of the data reported in this study have been corrected for the free-field response of the microphones.

The data from this study are divided into four groups to which the free-field corrections are applied. The corrections for 30° are applied to data taken at 20°, 30°, and 40°. Similarly, the corrections for 60°, 90°, and 120° are applied to data from 50°-70°, 80°-100°, and 110°-115°, respectively. In this manner a set of microphone corrected data is obtained by adding the appropriate free-field correction (in decibels) to each one-third octave band of the measured pressure. The free-field corrections used in this study are given in Table II.

As shown in figure 2 the microphone are positioned at different distances from the jet nozzle exit. All measured sound pressure levels are corrected to a distance of 3.05 m by adding a term of $20 \log_{10}(r/3.05)$ to the measured levels, where r is the measurement distance in meters from nozzle to the microphone (see Table I).

The acoustic data taken during a test condition with sonic jet in the presence of the wind tunnel flow contain components due to both jet noise and wind noise. Curve B of figure 12 shows the data from the in-wind microphone at an angle of 60° with a sonic jet and a wind tunnel speed of 42.7 m/s. Curve A shows the measured wind noise at a speed of 42.7 m/s (140 f/s). The sound pressure levels at the lower frequencies of Curve B are clearly dominated by wind noise while

Table II Free-field Microphone Corrections

One-third octave band center frequency	MICROPHONE CORRECTION (dB)			
	Angle ψ (degrees)			
	30	60	90	120
160	-0.40	-0.40	-0.40	-0.40
200	-0.40	-0.40	-0.40	-0.40
250	-0.40	-0.40	-0.40	-0.40
315	-0.40	-0.40	-0.40	-0.40
400	-0.40	-0.40	-0.40	-0.40
500	-0.40	-0.40	-0.40	-0.40
630	-0.40	-0.40	-0.40	-0.40
800	-0.40	-0.40	-0.40	-0.40
1,000	-0.40	-0.40	-0.40	-0.40
1,250	-0.40	-0.40	-0.40	-0.40
1,600	-0.40	-0.40	-0.40	-0.40
2,000	-0.40	-0.40	-0.40	-0.40
2,500	-0.40	-0.40	-0.40	-0.40
3,150	-0.40	-0.40	-0.40	-0.40
4,000	-0.25	0.05	0.25	0.25
5,000	-0.05	0.42	0.70	0.70
6,300	0.20	0.80	1.60	1.30
8,000	0.50	1.10	2.10	1.90
10,000	0.90	2.20	2.60	2.30
12,500	1.00	2.40	3.10	2.50
16,000	0.90	2.70	3.50	2.50
20,000	0.60	2.40	2.80	1.50
25,000	-1.40	0.30	0.60	0.50
31,500	-0.30	0.00	1.20	1.15
40,000	3.10	3.10	3.15	3.15
50,000	7.45	7.45	8.00	6.70
63,000	6.30	6.30	6.20	5.40

the sound pressure levels at the higher frequencies are influenced mainly by jet noise. At intermediate frequencies, however, the measured sound pressure levels are affected by both wind and jet noise. It is possible to remove to some extent the contributions of the wind noise from the jet noise spectra. This is done by logarithmically subtracting the one-third octave band levels of the wind noise from the levels of the jet noise in the presence of the wind. This process requires the reasonable assumption that the wind noise at a particular position and wind speed is repeatable. The result of this process gives the spectrum of the jet noise in the presence of the wind shown as Curve C on figure 12. This subtraction process is used to extend the low frequency limit of our data. In the following discussion all the jet noise data from the in-wind microphones in the presence of flow have been adjusted following the above method to remove the wind noise.

5.2 Presentation of Data

The wind noise measured by the in-wind microphones is generated by the wind tunnel flow over the nose cone, body, and support of the microphone. The in-wind microphones are oriented to point directly upstream into the flow. Measurements of the wind noise are made at locations in the potential core of the wind tunnel flow and for speeds of 30.5 m/s and 42.7 m/s (see Appendix A for wind noise data). The measured one-third octave band spectra for a wind speed of 42.7 m/s at locations corresponding to angles of 40° and 90° relative to the model jet (see geometry of figure 2) are shown on figure 13. The two spectra show similar behavior at low frequencies but somewhat different behavior at the higher frequencies. Differences in wind noise might be expected at various locations owing to variations in the hydrodynamic field of the wind tunnel flow. These variations occur in the frequency range where the noise of the model jet is dominant and therefore do not effect the interpretations of the jet noise data. Also shown on figure 13 is the spectrum for the wind noise of the UA 0385 nose cone provided by Brüel & Kjaer (ref. 24). This spectrum is for a wind speed of 44.6 m/s (146 f/s). The wind noise from reference 24 corresponding to a slightly greater wind speed is considerably greater than the wind noise measured in this study. Such differences in the level might result from different levels of turbulence in the flow and from different microphone support configurations. The spectra presented do however agree in general shape.

In the present study measurements of the noise from a sonic cold jet are made in the presence of wind with both in-wind and out-of-wind microphones (see Appendix B for jet noise data). The simultaneous measurement of jet noise using microphones in both locations is an unusual feature of the present study. As a result, the data must be compared separately with other experiments using out-of-wind microphones and with experiments using in-wind microphones.

Both Plumblee (ref. 6) and DeBelleval, et al (ref. 5) report data from a cold jet taken with <u>out-of-wind</u> microphones in a free-jet wind tunnel facility. In reference 6 the directivity of the overall sound pressure level is presented for a cold jet with an exit Mach number of 0.9 and flow Mach numbers of $M_o = 0.0^5$ and $M_o = 0.15$. Results are also reported in reference 5 for the directivity of the overall sound pressure level for a cold jet with an exit Mach number of 1.0. The Mach numbers of the wind tunnel flow are $M_o = 0.02$ and $M_o = .14$. The out-of-wind data from the present study for a sonic jet and flow Mach numbers of $M_o = 0.00$ and $M_o = 0.12$ are shown on figure 14 along with the results of references 5 and 6. The overall sound pressure levels of the present study include frequency components from 800 Hz to 63 KHz. The absolute levels for each of these three studies have been normalized by the addition of the term $-10 \log_{10} (\frac{A_j}{r^2})$ to account for individual differences in jet area and microphone distances. It should be noted that this correction is only approximate for noise data taken in the presence of flow. Refraction and scattering of the sound by the shear layer of the wind tunnel does not provide a sound field which scales directly with the inverse square of the distance from the source. The comparison of the overall sound pressure levels of static jet noise shows that there is some disagreement in absolute levels. The sound pressure levels reported in reference 6 are greater than those reported in reference 5 even though the Mach number of the jet in the latter study is greater (i.e. $M_j = 1.0$ compared with $M_j = 0.9$). The levels measured in the present study are as much as 4 dB greater than those reported in reference 5. This inconsistency in levels for the static jet noise may be due in part to non-anechoic characteristics of the individual facilities used. In the presence of wind, the three sets of jet noise data appear to show even less agreement. Compared with the overall sound pressure levels for static jet noise, the levels from the present study decrease by approximately 2.0 to 3.0 decibels with a flow of Mach number of $M_o = 0.12$. Similar decreases of 2.5 to 4.0 decibels are found for the data of references 5 and 6 with flow Mach numbers of approximately $M_o = 0.15$. It should be recalled that the out-of-wind data presented in figure 14 have only been corrected for the microphone response, exit area of the jet, and microphone distance. The effects of refraction and scattering of the sound by the turbulent shear layer of the wind tunnel are not accounted for. It would therefore be expected that there would be a substantial facility dependence of the data taken in the presence of the wind.

The directivity of the overall sound pressure level of sonic jet noise measured in the present study by the in-wind microphones is shown in figure 15. In this presentation the sound pressure levels are referred to the measured (i.e., reception) angle and are normalized to a constant measured (i.e., reception) distance of 3.05 m. The results are shown for flow Mach numbers of $M_o = 0.00$, 0.09, and 0.12. The level of the static jet noise is always greater than the corresponding level in the presence of flow. The difference in level tends to approach a constant value for reception angles greater than 90^o relative to the jet exit direction.

The data presented in figure 15 can be used to compare with theoretical predictions of the change in the source strength of jet noise owing to the presence of the wind tunnel flow. The source strength changes which correspond to the theoretical results of equations (1), (2), and (3) are expressed by calculating the quantity $10 \log_{10} \frac{S_j(V_j,0)}{S_j(V_j,V_o)}$, where $S_j(V_j,0)$ is the predicted source strength for static jet noise and $S_j(V_j,V_o)$ is the predicted source strength for jet noise in the presence of flow. The results of these three predictions for a cold sonic jet with wind speed of 42.7 m/s are presented in Table III. At an angle of 90^o where the

TABLE III. SOURCE STRENGTH CHANGE FOR M_j=1.0 and M_o=0.12

EQUATION	(1)	(2)	(3)
$10 \log_{10} \frac{S_j(V_j,0)}{S_j(V_j,V_o)}$	4.1dB	3.7dB	-0.6dB

effects of convection on sound propagation are expected to be minimal the data presented in figure 15 for M_o = 0.12 indicate a measured change in source strength of approximately 2.0dB. It therefore appears that equations (1) and (2) somewhat overpredict the measured change while equation (3) underpredicts the change in source strength.

The data from the in-wind microphones shown in figure 15 may also be presented in terms of the emission coordinates (R,θ) using the relationships of equations (4), (5), and (6). This presentation of the data from the present study for $M_o = 0.09$ and $R = 3.05$ m is shown in figure 16. Comparing with figure 15, the effect of presenting the data from the in-wind microphones in terms of the emission coordinates is seen to increase the level slightly and to shift the directivity pattern somewhat towards the larger angles. Also shown in figure 16 are the data from in-wind microphones reported by Cocking and Bryce (ref. 4). In the experimental procedure of reference 4, the microphone is located at a sideline distance of 2.16 m from the jet axis. The microphone is moved downstream as the flow speed increases so as to obtain the data directly in terms of emission coordinates. The data from reference 4 which appear in figure 16 have been adjusted to account for differences between the two studies in jet area and emission distance by adding the term $-10 \log_{10}\left(\frac{A_j}{R^2}\right)$ (where A_j and R are the exit area of the jet and the microphone distance respectively, used in the present study). While the same flow Mach numbers are used in the two studies ($M_o = 0.00$ and $M_o = 0.09$), the exit Mach number of the jet is $M_j = 1.0$ in the present study but $M_j = 0.84$ in reference 4. As shown in figure 16, there is a difference in overall sound pressure levels between the static jet noise of the two studies ranging from 7 dB to 3.5 dB at angles of 35° and 90°, respectively. The prediction method for static jet noise of reference 21 indicates that differences of approximately 7 dB and 5 dB at angles of 35° and 90°, respectively, should exist between sonic jet noise and the noise from a jet with Mach number 0.84. The results for static jet noise from the two studies are therefore in reasonably good agreement with each other.

The directivities of the overall sound pressure level of the jet noise in the presence of flow for the present study and for that of reference 4 are also shown in figure 16. In both cases the flow Mach number is $M_o = 0.09$. Compared with the level of static jet noise, the overall sound pressure level in the presence of the flow for the present study is reduced by 3.7 dB and 1.2 dB at angles of 30° and 90°, respectively. The reductions in level in the results from reference 4 at corresponding angles are 3.0 dB and 2.2 dB. Therefore, for the range of angles common to both studies, the trends of the data in the presence of flow are also found to be on reasonable agreement with each other.

Another common representation of the change in the directivity of the sound pressure level of jet noise in the presence of flow is the velocity exponent. The velocity exponent is defined as follows:

$$n(\theta) \equiv \frac{OASPL(V_j,0,\theta) - OASPL(V_j,V_o,\theta)}{10 \log_{10} \left(\frac{V_j}{V_j - V_o}\right)} \tag{12}$$

where $OASPL(V_j,0,\theta)$ and $OASPL(V_j,V_o,\theta)$ are the overall sound pressure levels at angle θ for static jet noise and for jet noise in the presence of flow, respectively. The sound pressure levels from the in-wind microphones of the present study are used to calculate the velocity exponent. Only the data in the limited frequency range of 1000 Hz to 6300 Hz have been used for this calculation in order to minimize those portions of the noise spectra which appear to be contaminated (see discussion in section 4.0). The velocity exponent calculated according to equation (12) from the present study (for $M_j = 1.0$ and $M_o = 0.09$) and from the data of reference 4 (for $M_j = 0.84$ and $M_o = 0.09$) is shown in figure 17. Except for the angles near the jet axis, the values and trends of the velocity exponent from the two studies are in reasonable agreement although the jet speeds are somewhat different in both studies. It should be noted that one disadvantage of presenting results in terms of the velocity exponent is the exaggeration of measurement uncertainties in sound pressure level. Since the velocity exponent is defined in terms of difference in sound pressure levels, it is a quantity which is sensitive to such uncertainties.

One of the features of the present study is the use of both in-wind and out-of-wind microphones to measure jet noise. It is to be expected that different assessments of the same jet noise will be made by both sets of microphones. As discussed in section 3.4 sound propagating through the turbulent shear layer of the wind tunnel flow will be refracted and scattered. A comparison of the jet noise data measured by the in-wind and out-of-wind microphones for a flow Mach number of

$M_o = 0.12$ is shown on figure 18. The sound pressure levels for both sets of data have been adjusted to a constant distance of 3.05 m assuming an inverse square law dependence on the distance from the source. Only the sound pressure levels from the limited range of frequencies (1000 Hz to 6300 Hz) have been included in this presentation. These data provide a means for testing the results of theoretical analyses of the effects of a shear layer on sound propagation. In particular, the data from the out-of-wind microphones have been adjusted, according to the analysis of Amiet (ref. 18). Since the theoretical analysis uses the model of a zero-thickness shear layer, the results of the analysis are independent of frequency. There should therefore be no difficulty with using the data in the limited frequency range for this comparison. This comparison is shown in figure 18. As can be seen, the data from the out-of-wind microphones which have been adjusted using the procedure of reference 18, are in reasonably good agreement with the data from the in-wind microphones. Although the agreement is not the same for all angles, the general trend of the adjusted data is reasonable.

6.0 CONCLUSIONS

The objective of this experimental study has been to measure the far-field characteristics of the noise from an unheated jet in the presence of a flow. Although experimental difficulties prevented total attainment of this objective, several aspects have been successfully completed. The conclusions which follow are based on these aspects of the study.

As indicated in Table III. there appears to be an inadequacy in the theoretical prediction of the effect of an external flow on the source strength of the noise from an unheated jet. The measured change in source strength appears to fall intermediate to the predictions of references 4 and 8 and of reference 9.

At all microphone positions in the present study, the overall sound pressure level of jet noise in the presence of flow is less than the level with no flow for the same jet speed (see figure 15). This is also found when the measured data are converted to equivalent flight data (figure 16). This result is consistent with that determined by Cocking and Bryce (ref. 4) with in-wind microphones for similar flow and jet conditions (see figure 16 and related discussion). It is important to reiterate that the results of both the present study and of reference 4 are obtained with an unheated jet.

The directivities of the overall sound pressure level of jet noise measured with out-of-wind microphones using different free-jet wind tunnels are not found to be in good agreement with each other (see figure 14). Agreement is poorest when there is a flow established in the wind tunnel. The lack of agreement of the static jet noise suggests that the free-jet wind tunnels are not behaving as purely anechoic test facilities. This is not completely surprising owing to the proximity of the wind tunnel nozzle to the model jet. The deterioration of the agreement when flow is established emphasizes the dependence of the noise measured outside the flow on the geometry and on the nature of the shear-layer of the wind tunnel flow.

In the present study the jet noise is measured independently with microphones located both inside and outside of the wind tunnel flow. Based on those portions of the data which appear to be uncontaminated (see discussion of section 4.0), the theory of Amiet (ref. 18) provides a substantial portion of the adjustment necessary to "correct" the out-of-wind data to equivalent in-wind conditions (see fig. 18). It should be emphasized that this comparison does not constitute a definitive test of this theory of sound propagation through a shear layer. The detailed experimental results of reference 17 suggest that the effects of forward scattering of sound by turbulence in the shear layer are also important.

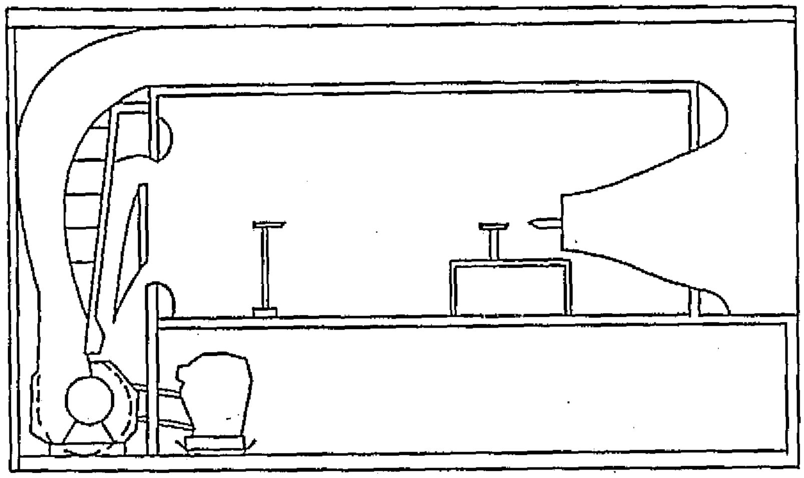

(A)

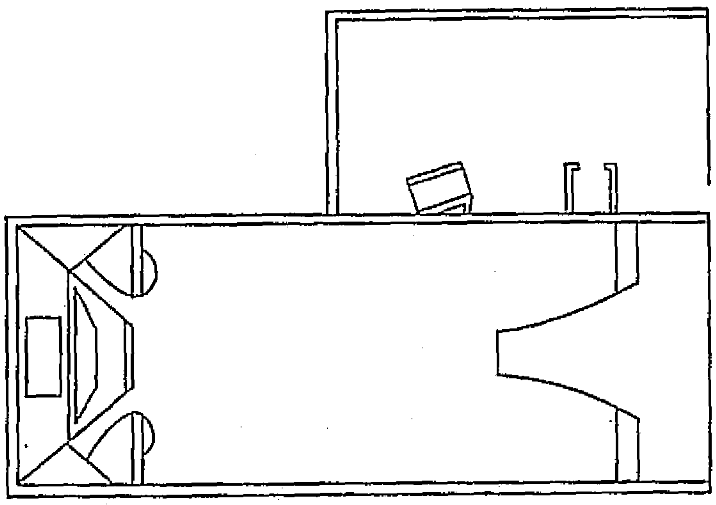

(B)

Figure 1. Elevation (A) and Plan (B) views of the free-jet wind tunnel facility from ref. 7. (Approximate scale = 1:200.)

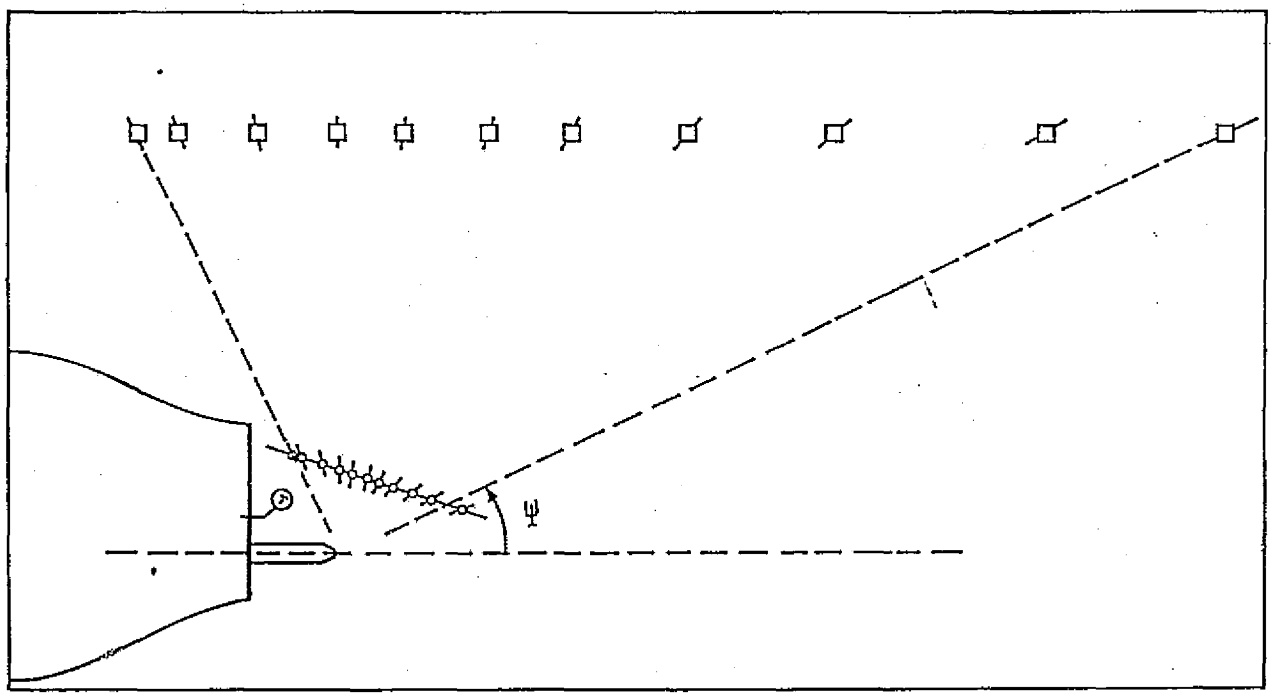

Figure 2. Locations of the in-wind (0) and out-of-wind (□) microphones and of the pitot tube for the wind tunnel flow.

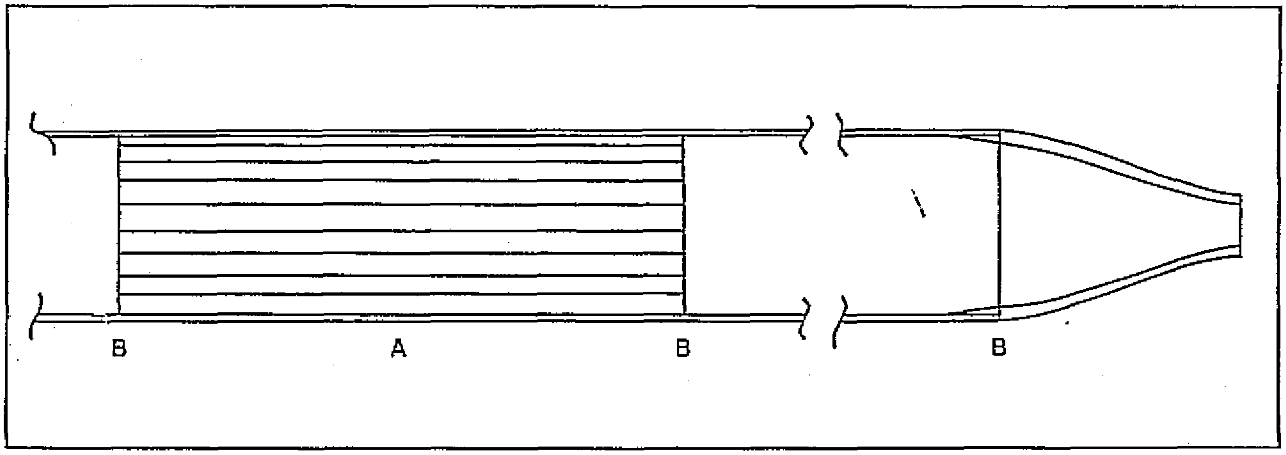

Figure 3. Detail of model jet indicating flow straighteners (A) and screens (B).

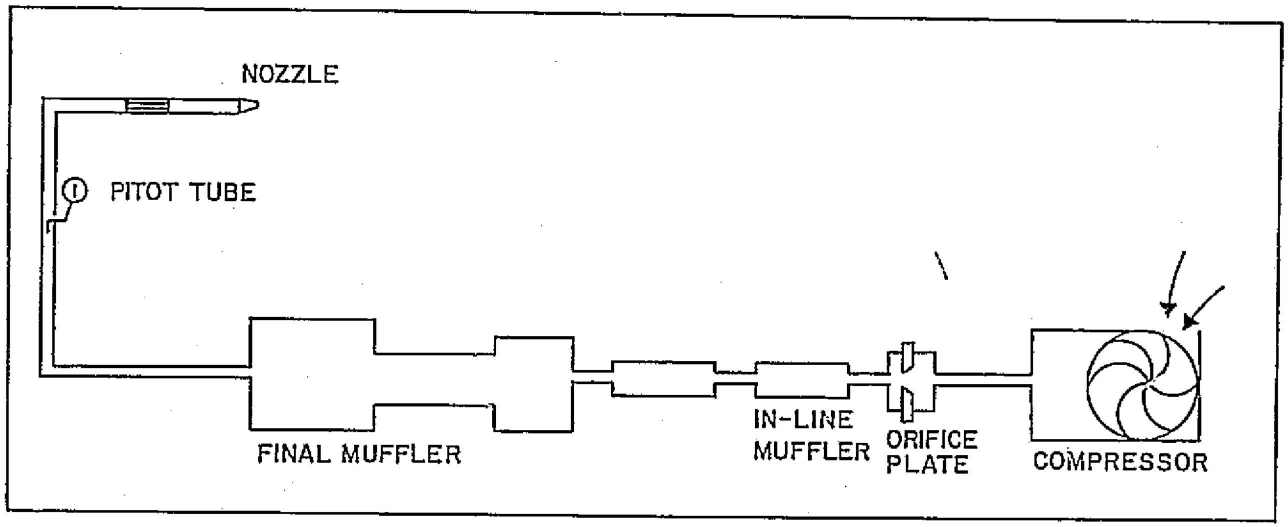

Figure 4. Diagram of the air supply for the model jet.

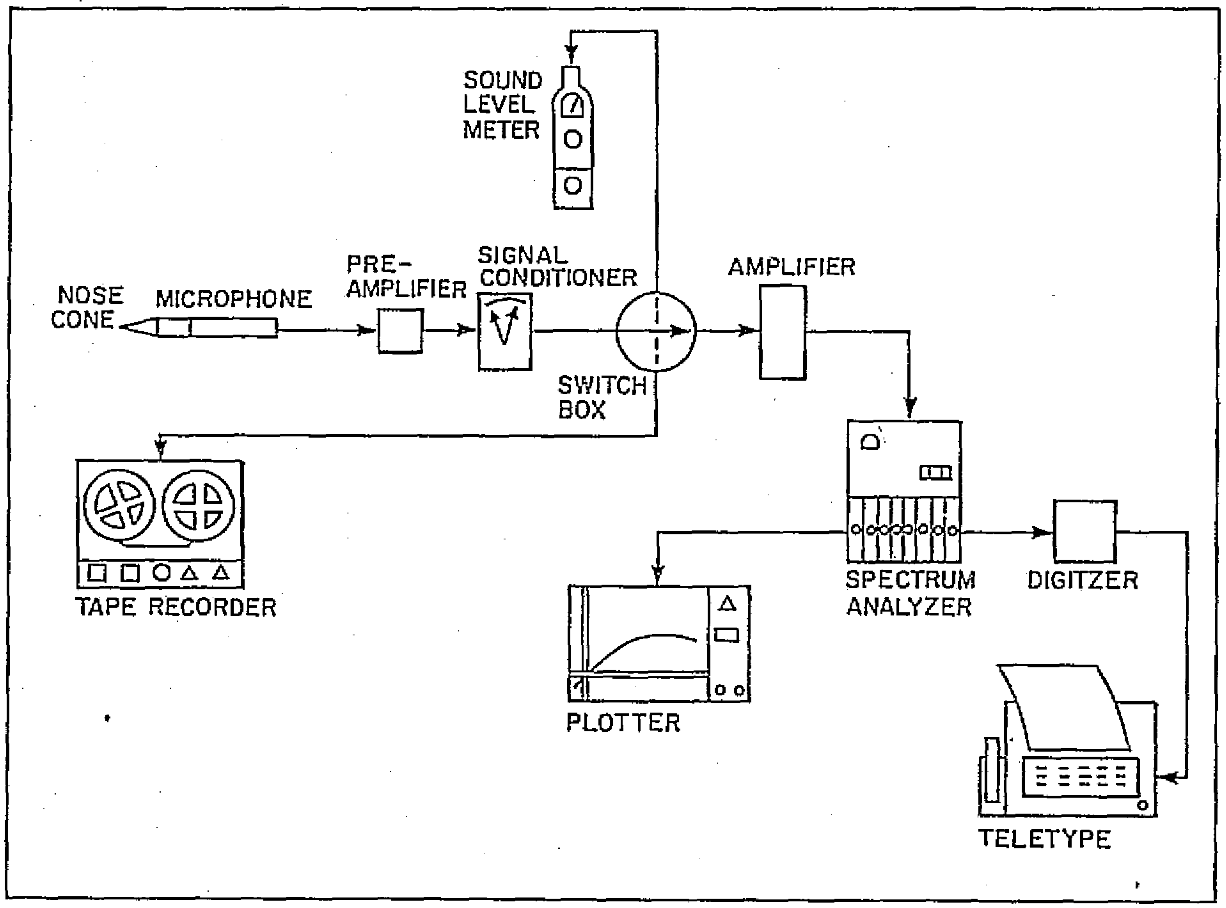

Figure 5. Diagram of the electrical instrumentation.

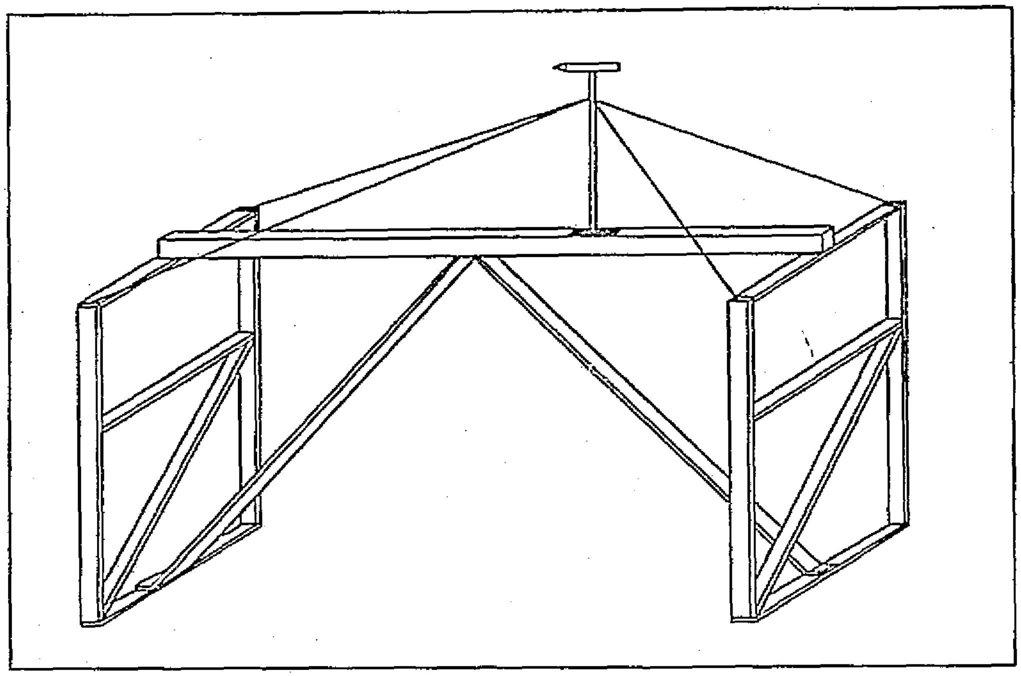

Figure 6. Support structure for the in-wind microphone.

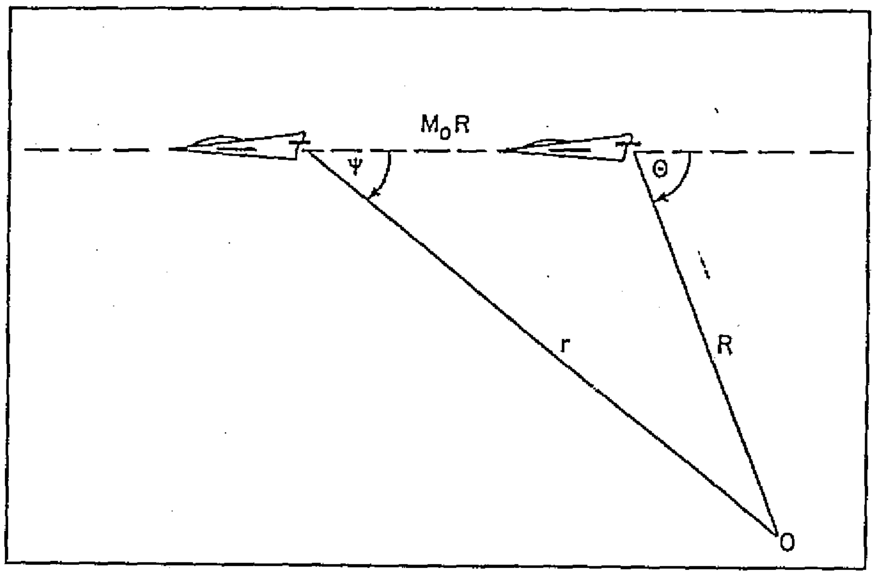

Figure 7. Relationship between emission and reception coordinate systems.

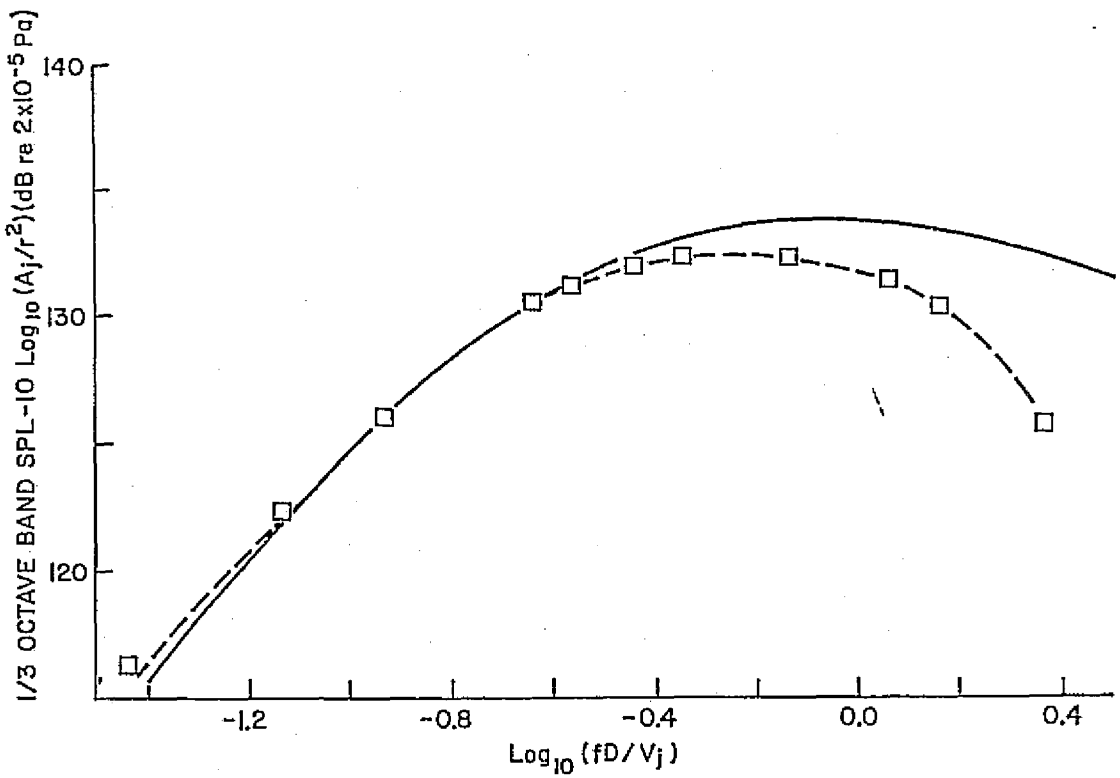

Figure 8. One-third octave band spectrum of the sound pressure level of sonic jet noise at an angle of 60° relative to the jet exit direction. (□--□, data measured at the out-of-wind microphone location; ——, spectrum predicted from reference 21.)

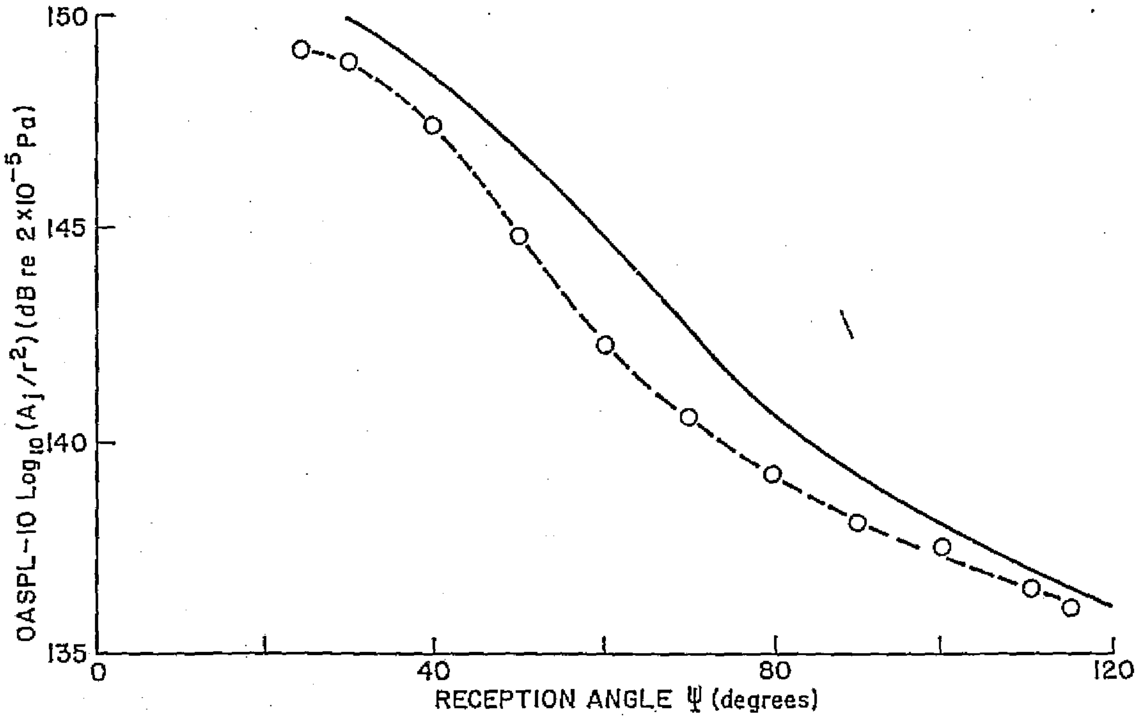

Figure 9. Directivity of the overall sound pressure level of sonic jet noise. (0--0, data measured at the out-of-wind microphone locations; ——. directivity predicted from reference 21.)

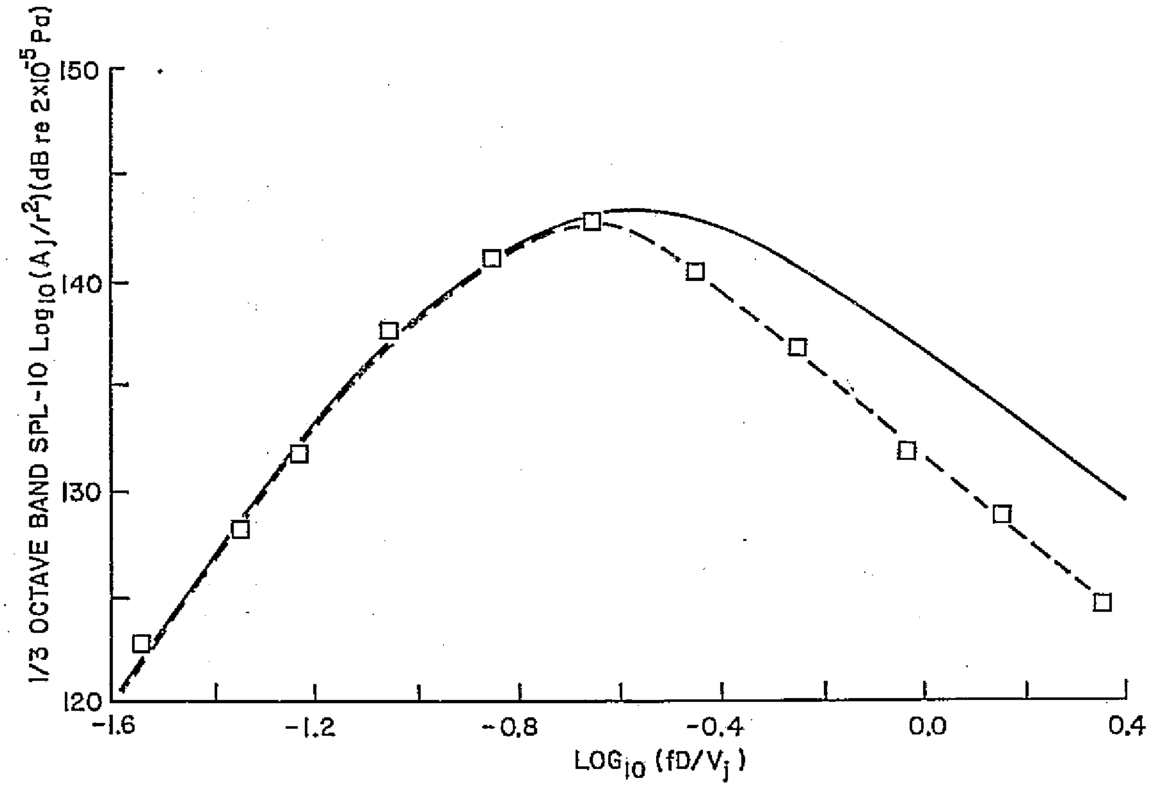

Figure 10. One-third octave band spectrum of the sound pressure level of sonic jet noise at an angle of 30° relative to the jet exit direction. (□--□, data measured at the in-wind microphone location; ——, spectrum predicted from reference 22.)

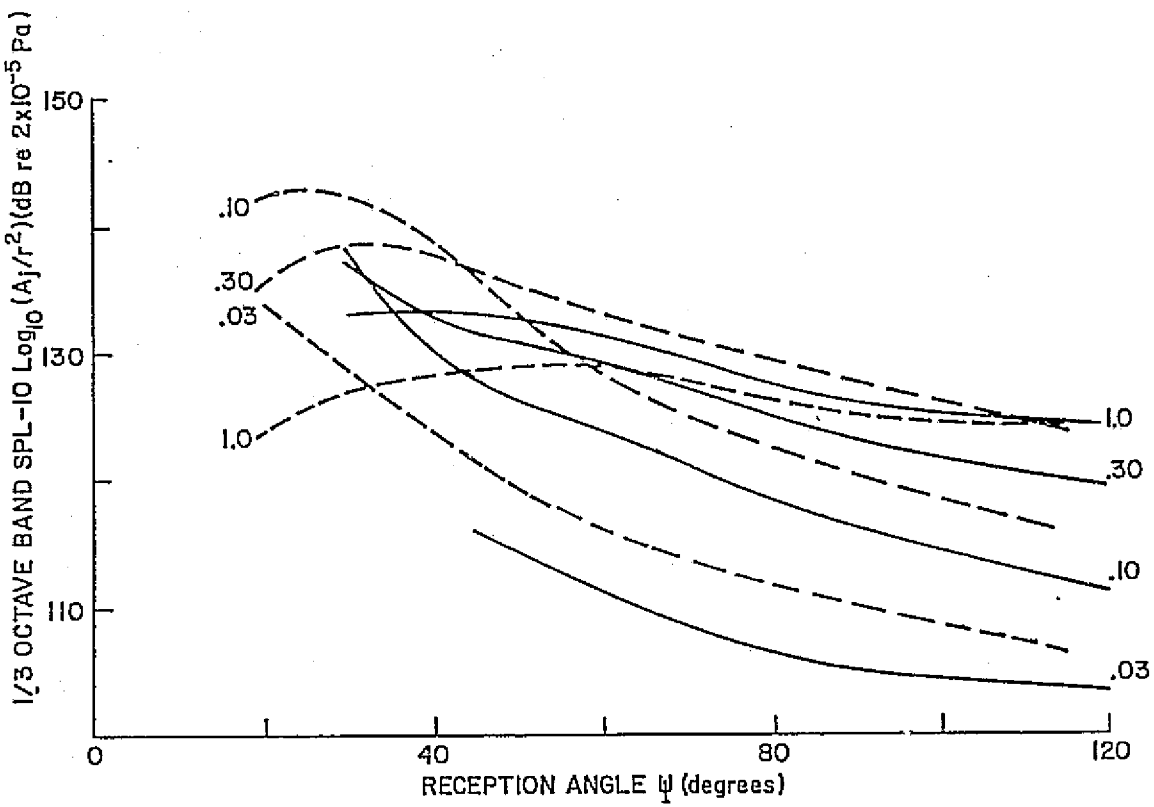

Figure 11. Comparison of the directivity of the sound pressure level of jet noise in one-third octave bands for different values of the Doppler corrected Strouhal number: $S_{d.c.} = \frac{f\, d_j\, (1-M_c \cos\psi)}{V_j}$. (---- , data measured at the in-wind microphone locations for $M_j = 1.0$; —— , data reported in reference 15 for $M_j = 0.9$.)

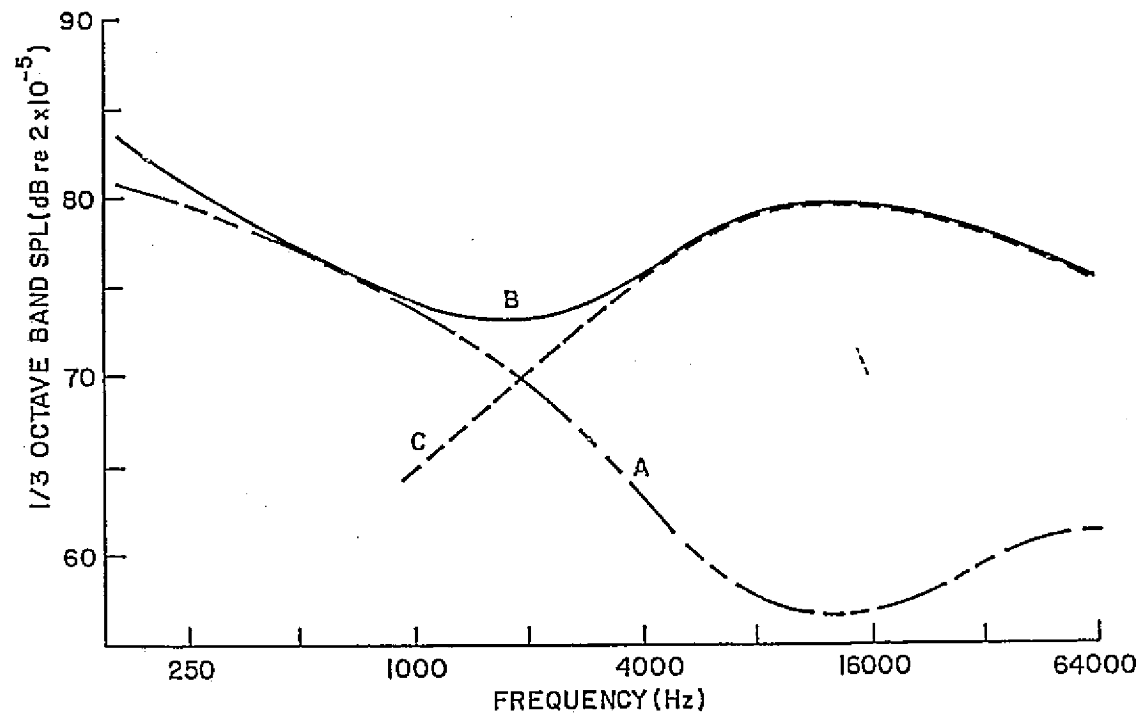

Figure 12. One-third octave band spectrum of measured wind noize (A), measured jet noise in the presence of wind (B), and resulting jet noise in the presence of wind after subracting the wind noise contribution (C). Data measured at $\psi = 60^o$, $r = 3.05m$ with $M_j = 1.0$ and $M_o = 0.12$.

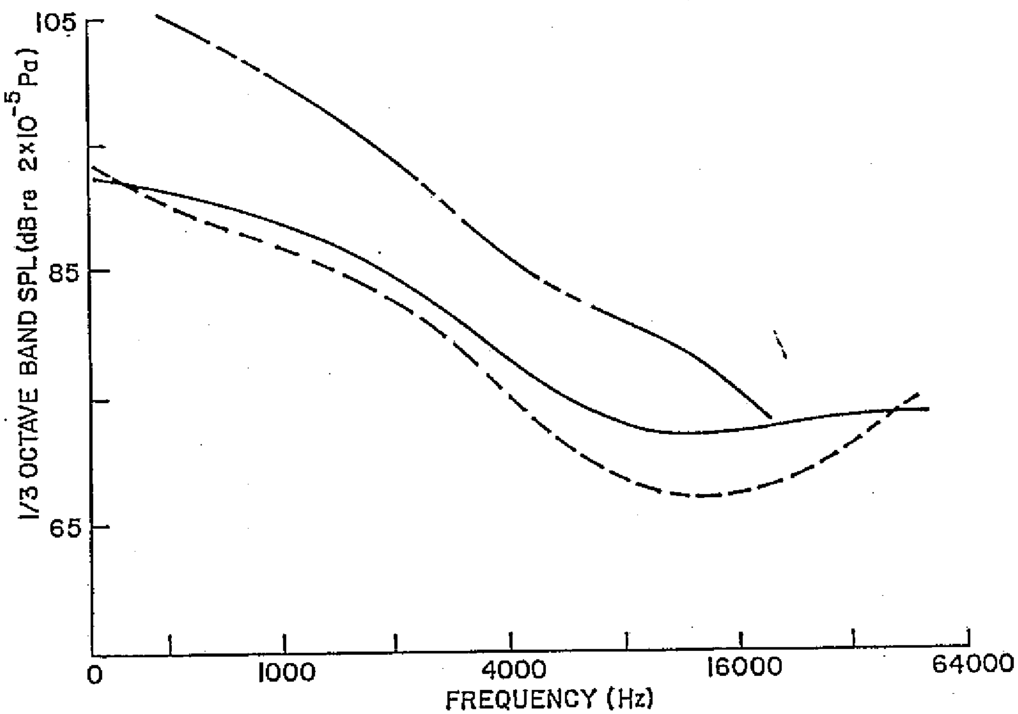

Figure 13. One-third octave band spectrum of the sound pressure level of microphone wind noise. (--- , data measured by the in-wind microphone at 40° with V_o = 42.7 m/s; ——, data measured by the in-wind microphone at 90° with V_o = 42.7 m/s; —-——, data reported in reference 24 with V_o = 44.6 m/s.

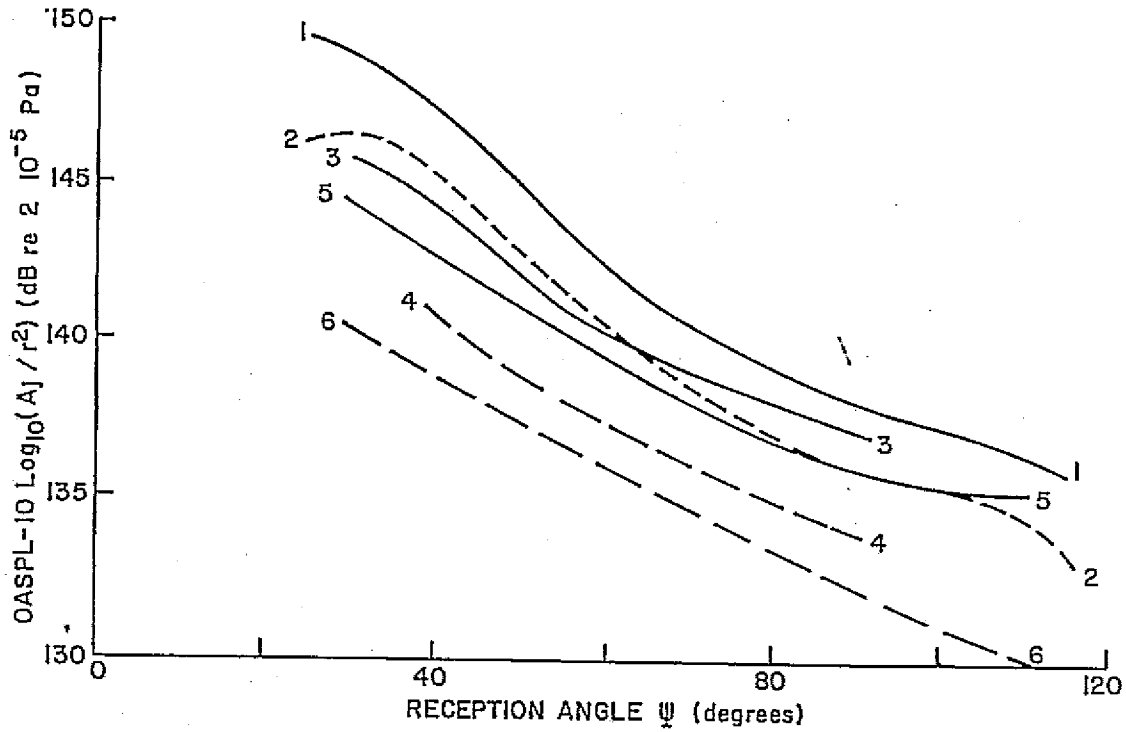

Figure 14. Directivity of the overall sound pressure level of jet noise with and without external flow. All data measured by out-of-wind microphones. (Data from the present study with $M_j = 1.0$ and $M_o = 0.0$ (1—1), $M_o = 0.12$ (2---2); data from reference 6 with $M_j = 0.9$ and $M_o = 0.05$ (3—3), $M_o = 0.15$ (4--4); data from reference 5 with $M_j = 1.0$ and $M_o = 0.02$ (5—5), $M_o = 0.14$ (6--6).)

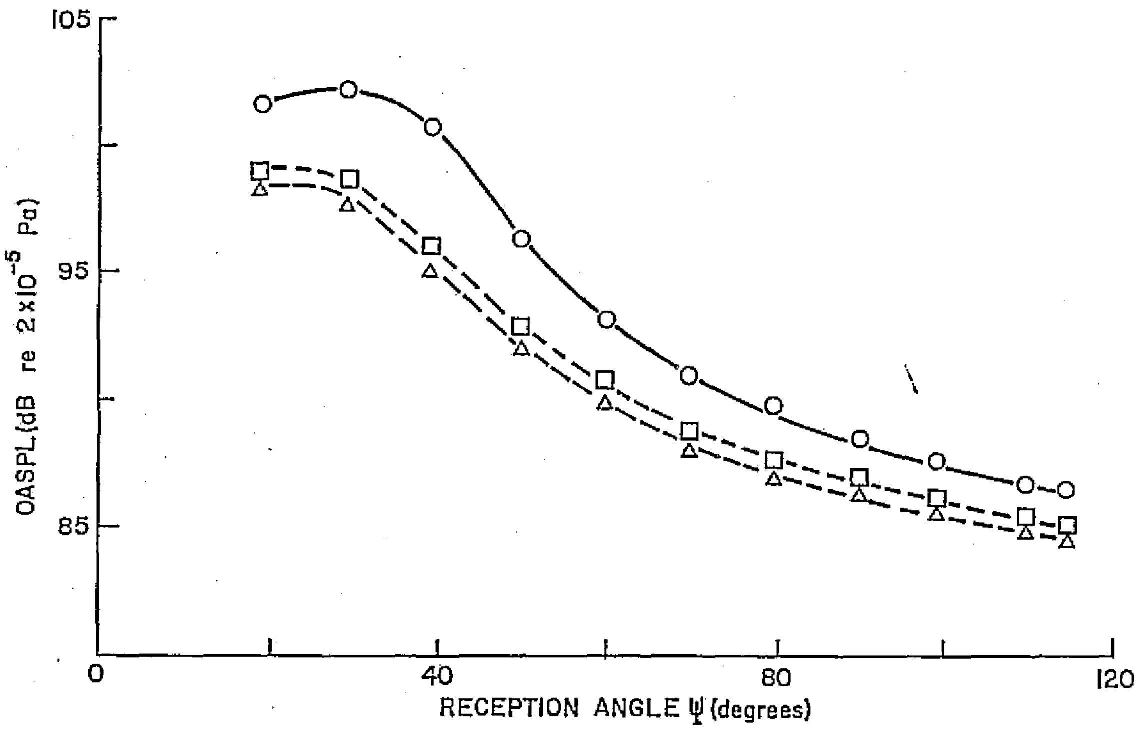

Figure 15. Directivity of the overall sound pressure level of sonic jet noise with and without external flow measured in the present study by in-wind microphones. (0—0, $M_o = 0.00$; □---□, $M_o = 0.09$; Δ---Δ, $M_o = 0.12$.)

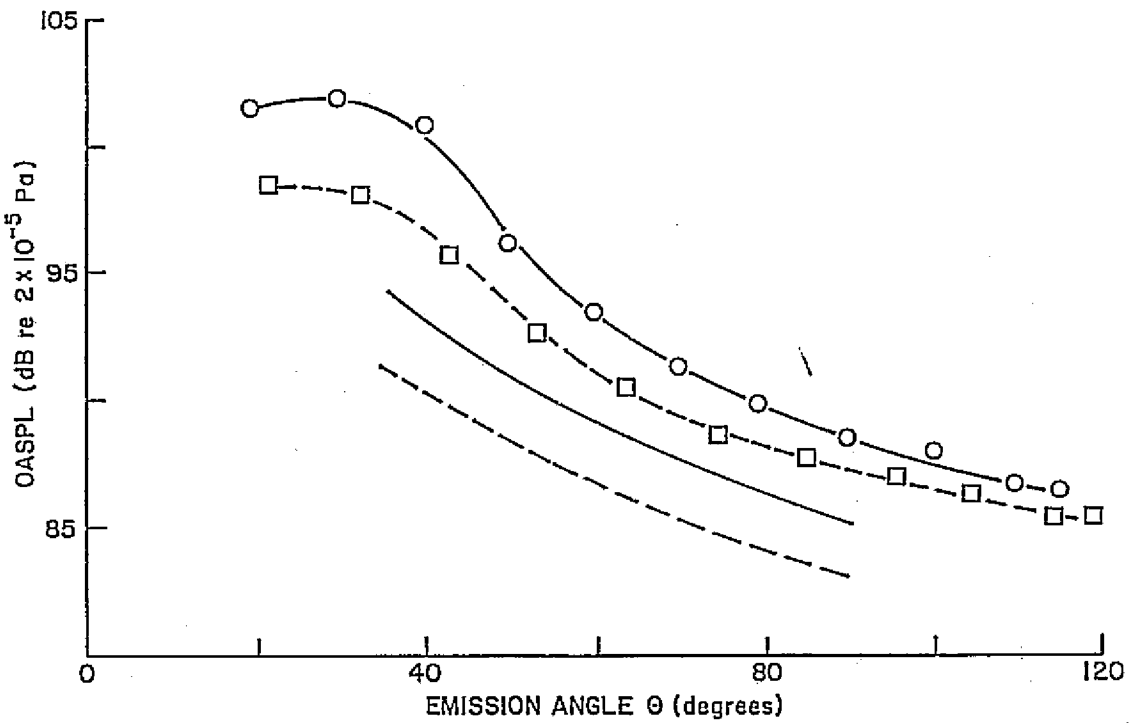

Figure 16. Directivity of the overall sound pressure level of jet noise with and without external flow in terms of emission coordinates. Data are measured with in-wind microphones and normalized to a distance of 3.05 m. (Data from the present study with $M_j = 1.0$ and $M_o = 0.00$ (O—O), $M_o = 0.09$ (□--□); data from reference 4 with $M_j = 0.84$ and $M_o = 0.02$ (——), $M_o = 0.09$ (---) .)

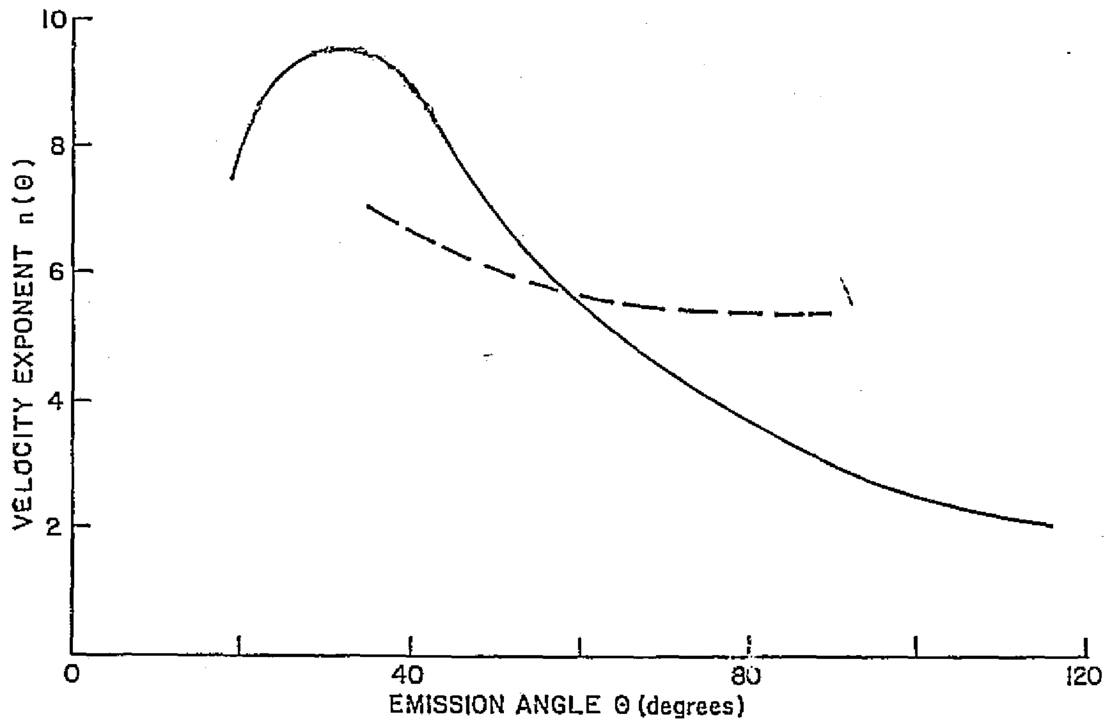

Figure 17. Velocity exponent based on data from in-wind microphones. (—— , data from the present study in the frequency range of 1000 to 6300 Hz with $M_j = 1.0$ and $M_o = 0.09$; --- , data from reference 4 with $M_j = 0.84$ and $M_o = 0.09$.)

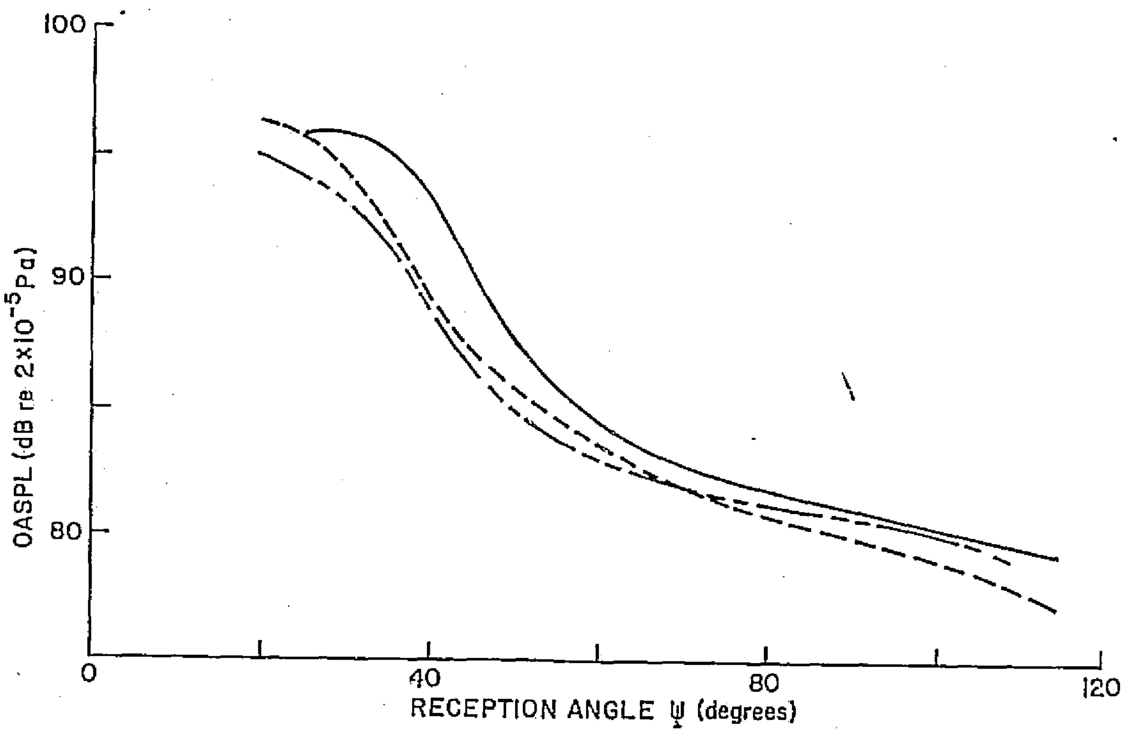

Figure 18. Directivity of the sound pressure level of jet noise measured by in-wind and out-of-wind microphones for $M_j = 1.0$ and $M_o = 0.12$. Sound pressure levels are normalized to a distance of 3.05m and are based on the frequency range of 1000 to 6300 Hz. (——, out-of-wind data; — ——— , in-wind data; --- , out-of-wind data adjusted to in-wind conditions using the method of reference 18.)

APPENDIX A

WIND NOISE MEASURED AT THE IN-WIND MICROPHONE LOCATIONS FOR SPEEDS OF 30.5 m/s and 42.7 m/s. (DATA CORRECTED FOR MICROPHONE RESPONSE.)

WIND NOISE

$V_o = 30.5$ m/s $(M_o = 0.09)$

$V_j = 0.00$

one-third octave band center frequency	1/3 octave band SPL - dB(re 2×10^{-5}Pa)		
	Angle ψ (degrees)		
	115	110	100
160.00	84.85	90.35	85.35
200.00	84.60	90.60	85.35
250.00	84.60	88.10	85.35
315.00	83.35	85.85	84.60
400.00	83.35	84.60	84.35
500.00	82.35	83.85	83.60
630.00	82.10	83.10	82.60
800.00	81.10	82.10	82.35
1000.00	79.60	80.60	80.60
1250.00	77.60	78.60	78.35
1600.00	75.60	76.35	76.10
2000.00	72.60	73.85	73.35
2500.00	69.85	71.35	70.85
3150.00	66.35	67.60	67.60
4000.00	63.50	63.75	64.00
5000.00	62.45	62.45	62.70
6300.00	63.55	63.55	65.85
8000.00	63.90	63.40	65.35
10000.00	65.55	65.05	66.60
12500.00	65.75	66.00	68.35
16000.00	64.50	64.50	66.50
20000.00	65.25	67.25	65.80
25000.00	64.50	65.00	65.35
31500.00	70.65	70.90	71.70
40000.00	70.90	70.90	71.90
50000.00	67.20	66.95	70.75
63000.00	65.40	65.40	66.20
OASPL	93.12	96.53	94.01

WIND NOISE

$V_o = 30.5$ m/s ($M_o = 0.09$)

$V_j = 0.00$

one-third octave band center frequency	1/3 octave band SPL - dB(re $2x10^{-5}$Pa)		
	Angle ψ (degrees)		
	90	80	70
160.00	85.85	93.55	93.35
200.00	85.10	92.80	92.60
250.00	84.85	90.05	89.85
315.00	84.85	88.30	88.10
400.00	84.35	86.30	86.10
500.00	83.60	85.30	85.10
630.00	82.85	84.80	84.60
800.00	82.35	83.30	83.10
1000.00	80.60	82.55	82.35
1250.00	79.10	80.30	80.10
1600.00	76.85	77.55	77.35
2000.00	74.10	75.05	74.85
2500.00	71.60	72.80	72.60
3150.00	67.85	68.80	68.60
4000.00	64.75	65.25	65.05
5000.00	63.45	63.37	63.17
6300.00	65.35	63.75	63.55
8000.00	64.85	62.80	62.60
10000.00	65.35	64.90	64.70
12500.00	67.60	67.10	66.90
16000.00	65.25	65.63	65.43
20000.00	64.55	66.10	65.90
25000.00	63.85	65.00	64.80
31500.00	70.45	71.45	71.25
40000.00	71.15	71.80	71.60
50000.00	70.00	67.65	67.45
63000.00	66.20	66.50	66.30
OASPL	94.05	98.82	98.61

WIND NOISE

$V_o = 30.5$ m/s ($M_o = 0.09$)

$V_j = 0.00$

one-third octave band center frequency	1/3 octave band SPL - dB(re 2×10^{-5}Pa)		
	Angle ψ (degrees)		
	60	50	40
160.00	92.73	91.13	90.85
200.00	91.98	97.13	96.85
250.00	89.23	94.63	94.35
315.00	87.48	85.63	85.35
400.00	85.48	84.63	84.35
500.00	84.48	83.63	83.35
630.00	83.98	83.63	83.35
800.00	82.48	82.38	82.10
1000.00	81.73	81.13	80.85
1250.00	79.48	78.88	78.60
1600.00	76.73	76.13	75.85
2000.00	74.23	74.38	74.10
2500.00	71.98	70.88	70.60
3150.00	67.98	67.13	66.85
4000.00	64.43	63.03	62.75
5000.00	62.55	61.48	61.20
6300.00	62.93	63.22	62.95
8000.00	61.98	61.78	61.50
10000.00	64.08	63.93	63.65
12500.00	66.28	66.03	65.75
16000.00	64.81	63.43	63.15
20000.00	65.28	62.38	62.10
25000.00	64.18	63.38	33.10
31500.00	70.63	73.48	73.20
40000.00	70.98	74.88	74.60
50000.00	66.83	71.22	69.95
63000.00	65.68	69.83	68.55
OASPL	98.00	100.43	100.15

WIND NOISE

$V_o = 30.5$ m/s ($M_o = 0.09$)

$V_j = 0.00$

one-third octave band center frequency	1/3 octave band SPL - dB(re $2x10^{-5}$Pa)		
	Angle ψ (degrees)		
	30	20	
160.00	89.91	85.35	
200.00	95.91	84.60	
250.00	93.40	83.60	
315.00	84.40	83.10	
400.00	83.40	82.60	
500.00	82.40	81.35	
630.00	82.40	81.35	
800.00	81.15	79.35	
1000.00	79.91	78.10	
1250.00	77.65	76.10	
1600.00	74.91	73.85	
2000.00	73.15	70.60	
2500.00	69.65	68.60	
3150.00	65.91	64.60	
4000.00	61.80	61.25	
5000.00	59.25	59.95	
6300.00	62.01	61.70	
8000.00	60.55	60.50	
10000.00	62.70	62.90	
12500.00	64.80	64.50	
16000.00	62.20	60.90	
20000.00	61.15	60.60	
25000.00	31.15	60.60	
31500.00	72.25	72.95	
40000.00	73.65	73.85	
50000.00	69.01	69.95	
63000.00	67.60	68.55	
OASPL	99.20	92.62	

WIND NOISE

V_o = 42.7 m/s (M_o = 0.12)

V_j = 0.00

one-third octave band center frequency	1/3 octave band SPL - dB(re $2x10^{-5}$Pa)		
	Angle ψ (degrees)		
	115	110	100
160.00	93.10	97.35	93.10
200.00	92.60	96.10	93.85
250.00	92.35	93.35	92.85
315.00	92.60	92.35	92.10
400.00	91.10	91.60	91.35
500.00	90.60	90.35	89.85
630.00	90.10	89.60	90.10
800.00	89.35	89.10	88.35
1000.00	88.10	88.10	88.10
1250.00	87.10	87.10	86.60
1600.00	85.60	85.35	85.35
2000.00	84.10	83.60	83.60
2500.00	82.10	82.10	81.85
3150.00	80.10	79.85	79.85
4000.00	78.25	77.25	77.25
5000.00	74.95	74.45	73.95
6300.00	72.30	71.80	71.60
8000.00	71.90	71.90	70.85
10000.00	73.30	73.05	72.60
12500.00	73.75	73.25	73.10
16000.00	72.75	72.00	72.25
20000.00	74.00	74.25	74.80
25000.00	74.00	74.50	74.60
31500.00	73.90	74.15	72.95
40000.00	73.90	73.90	73.15
50000.00	71.70	71.45	72.00
63000.00	68.15	68.15	67.95
OASPL	101.48	102.99	101.54

WIND NOISE

$V_o = 42.7$ m/s ($M_o = 0.12$)

$V_j = 0.00$

one-third octave band center frequency	1/3 octave band SPL - dB(re $2x10^{-5}$Pa)		
	Angle ψ (degrees)		
	90	80	70
160.00	94.35	96.05	95.85
200.00	93.85	94.80	94.60
250.00	93.10	94.30	94.10
315.00	92.60	93.05	92.85
400.00	92.10	92.55	92.35
500.00	90.85	91.80	91.60
630.00	90.35	91.30	91.10
800.00	89.85	90.30	90.10
1000.00	88.85	89.30	89.10
1250.00	87.85	87.80	87.60
1600.00	85.85	86.55	86.35
2000.00	84.35	84.30	84.10
2500.00	83.10	83.30	83.10
3150.00	80.85	81.05	80.85
4000.00	78.25	78.50	78.30
5000.00	75.20	75.37	75.17
6300.00	72.10	72.00	71.80
8000.00	72.10	71.30	71.10
10000.00	73.10	72.90	72.70
12500.00	72.85	73.10	72.90
16000.00	72.25	71.88	71.68
20000.00	74.80	74.60	74.40
25000.00	74.60	75.00	74.80
31500.00	73.95	73.20	73.00
40000.00	74.15	74.05	73.85
50000.00	73.25	72.15	71.95
63000.00	68.95	69.00	68.80
DASPL	102.20	103.08	102.88

<u>WIND NOISE</u>

$V_o = 42.7$ m/s ($M_o = 0.12$)

$V_j = 0.00$

one-third octave band center frequency	1/3 octave band SPL - dB(re 2×10^{-5}Pa)		
	Angle ψ (degrees)		
	60	50	40
160.00	95.23	102.88	102.60
200.00	93.98	108.88	108.60
250.00	93.48	106.63	106.35
315.00	92.23	95.38	95.10
400.00	91.73	92.38	92.10
500.00	90.98	90.12	89.85
630.00	90.48	89.63	89.35
800.00	89.48	89.12	88.85
1000.00	88.48	87.88	87.60
1250.00	86.98	86.12	85.85
1600.00	85.73	85.12	84.85
2000.00	83.48	83.12	82.85
2500.00	82.48	81.38	81.10
3150.00	80.23	79.12	78.85
4000.00	77.68	75.52	75.25
5000.00	74.55	71.73	71.45
6300.00	71.18	68.73	68.45
8000.00	70.48	68.03	67.75
10000.00	72.08	69.17	68.90
12500.00	72.28	69.52	69.25
16000.00	71.06	68.17	67.90
20000.00	73.78	67.38	67.10
25000.00	74.18	67.63	67.35
31500.00	72.38	74.73	74.45
40000.00	73.23	76.12	75.85
50000.00	71.33	73.73	73.45
63000.00	68.18	71.83	71.55
OASPL	102.26	111.84	111.56

WIND NOISE

$V_o = 42.7$ m/s ($M_o = 0.12$)

$V_j = 0.00$

one-third octave band center frequency	1/3 octave band SPL – dB(re 2×10^{-5}Pa)		
	Angle ψ (degrees)		
	30	20	
160.00	101.65	108.60	
200.00	107.65	109.10	
250.00	105.40	103.85	
315.00	94.15	98.60	
400.00	91.15	96.60	
500.00	88.91	93.10	
630.00	88.40	90.35	
800.00	87.91	89.10	
1000.00	86.65	87.85	
1250.00	84.91	86.35	
1600.00	83.91	85.10	
2000.00	81.91	82.60	
2500.00	80.15	81.10	
3150.00	77.91	78.35	
4000.00	74.31	75.25	
5000.00	70.50	72.45	
6300.00	67.50	68.95	
8000.00	66.80	69.25	
10000.00	67.96	69.40	
12500.00	68.31	69.25	
16000.00	66.96	67.40	
20000.00	66.15	66.35	
25000.00	66.40	67.10	
31500.00	73.50	73.70	
40000.00	74.91	74.85	
50000.00	72.50	72.20	
63000.00	70.60	69.80	
OASPL	110.60	112.91	

APPENDIX B

JET NOISE MEASUREMENTS. (DATA CORRECTED FOR MICROPHONE RESPONSE AND ADJUSTED TO A DISTANCE OF 3.05m.)

JET NOISE

Out-of-Wind Microphone

Angle $\psi = 25^{o}$

$V_j = 340$ m/s ($M_j = 1.0$)

one-third octave band center frequency	1/3 octave band SPL - dB(re $2x10^{-5}$Pa)		
	wind speed - V_o (m/s)		
	0.00	30.5	42.7
160.00	65.14	72.89	78.89
200.00	65.14	70.64	77.39
250.00	65.14	69.14	75.14
315.00	65.89	67.39	73.39
400.00	67.39	66.14	70.89
500.00	69.14	65.89	68.39
630.00	72.64	68.64	68.39
800.00	75.14	70.89	69.64
1000.00	78.14	74.14	72.64
1250.00	81.14	78.14	76.39
1600.00	84.14	80.64	79.14
2000.00	86.64	83.89	82.64
2500.00	89.39	87.14	85.39
3150.00	90.64	88.89	87.64
4000.00	91.29	89.29	89.04
5000.00	92.49	90.49	89.49
6300.00	91.99	90.49	88.99
8000.00	91.29	89.29	88.04
10000.00	89.19	87.19	85.19
12500.00	86.79	85.04	82.29
16000.00	84.44	81.94	80.69
20000.00	82.89	81.14	80.14
25000.00	80.89	79.39	77.14
31500.00	80.24	78.99	77.49
40000.00	82.39	82.14	81.64
50000.00	79.99	79.24	79.24
63000.00	71.84	71.84	71.84
OASPL	100.56	98.64	97.54

JET NOISE

Out-of-Wind Microphone

Angle $\psi = 30^{\circ}$

$V_j = 340$ m/s ($M_j = 1.0$)

one-third octave band center frequency	1/3 octave band SPL - dB(re 2×10^{-5}Pa)		
	wind speed - V_o (m/s)		
	0.00	30.5	42.7
160.00	63.68	64.00	68.43
200.00	63.68	64.00	66.68
250.00	63.68	64.00	63.93
315.00	63.93	64.00	63.93
400.00	65.68	64.00	63.68
500.00	68.68	66.00	65.43
630.00	71.18	68.00	67.18
800.00	74.18	70.18	68.68
1000.00	77.43	73.68	72.93
1250.00	80.18	77.18	76.18
1600.00	82.68	79.93	78.93
2000.00	85.68	83.43	82.68
2500.00	88.43	85.68	85.43
3150.00	90.18	87.68	87.43
4000.00	91.83	89.33	88.83
5000.00	92.28	89.78	90.28
6300.00	92.03	90.78	90.03
8000.00	90.83	89.33	89.08
10000.00	88.98	87.73	86.73
12500.00	86.58	85.33	84.08
16000.00	84.23	82.48	82.73
20000.00	82.93	80.68	81.18
25000.00	80.68	78.18	78.18
31500.00	80.78	77.53	77.78
40000.00	81.43	80.93	80.68
50000.00	79.03	78.28	79.03
63000.00	72.13	70.88	72.88
OASPL	100.30	98.31	97.99

JET NOISE

Out-of-Wind Microphone

Angle $\psi = 40^{o}$

$V_j = 340$ m/s $(M_j = 1.0)$

one-third octave band center frequency	1/3 octave band SPL - dB(re $2x10^{-5}$Pa)		
	wind speed - V_o (m/s)		
	0.00	30.5	42.7
160.00	59.50	65.75	65.25
200.00	60.75	61.50	62.75
250.00	57.65	61.50	61.50
315.00	61.75	61.50	61.75
400.00	62.75	61.50	61.75
500.00	65.25	63.00	62.50
630.00	68.00	65.50	64.25
800.00	70.50	67.50	66.50
1000.00	73.50	70.75	70.00
1250.00	76.50	74.00	73.25
1600.00	79.25	76.50	75.75
2000.00	82.25	80.00	79.25
2500.00	85.00	82.75	81.50
3150.00	87.25	84.75	84.00
4000.00	88.40	86.15	85.65
5000.00	89.60	88.10	87.85
6300.00	89.60	88.35	88.35
8000.00	89.65	88.15	88.15
10000.00	89.05	87.30	87.30
12500.00	87.15	85.90	85.65
16000.00	86.05	84.05	83.80
20000.00	85.00	83.25	82.75
25000.00	83.00	80.75	80.50
31500.00	82.85	80.60	80.60
40000.00	81.75	81.25	81.50
50000.00	79.60	79.10	79.10
63000.00	75.20	74.95	74.45
OASPL	98.65	96.95	96.71

JET NOISE

Out-of-Wind Microphone

Angle $\psi = 50^{o}$

$V_j = 340$ m/s $(M_j = 1.0)$

one-third octave band center frequency	1/3 octave band SPL - dB(re $2x10^{-5}$Pa)		
	wind speed - V_o (m/s)		
	0.00	30.5	42.7
160.00	58.48	60.48	64.48
200.00	58.23	61.23	63.48
250.00	59.98	59.98	62.23
315.00	59.98	61.23	61.98
400.00	59.98	60.98	62.23
500.00	61.98	61.73	61.48
630.00	64.23	62.98	63.98
800.00	66.73	64.48	66.73
1000.00	69.23	67.23	66.23
1250.00	72.48	72.23	68.98
1600.00	74.73	72.98	70.73
2000.00	76.98	74.48	73.23
2500.00	79.48	76.48	75.73
3150.00	81.48	78.98	77.98
4000.00	82.68	80.93	80.18
5000.00	84.55	82.80	82.05
6300.00	85.68	83.93	83.18
8000.00	86.98	84.73	83.98
10000.00	86.83	85.33	84.58
12500.00	85.78	84.03	84.78
16000.00	85.81	83.81	83.31
20000.00	85.53	83.53	83.53
25000.00	84.68	81.93	81.93
31500.00	83.63	81.13	81.13
40000.00	81.73	79.98	80.48
50000.00	79.58	78.08	78.83
63000.00	76.68	75.93	75.68
OASPL	96.12	94.17	93.85

<u>JET NOISE</u>

Out-of-Wind Microphone
Angle $\psi = 60^{\circ}$

$V_j = 340$ m/s ($M_j = 1.0$)

one-third octave band center frequency	1/3 octave band SPL - dB(re 2×10^{-5}Pa)		
	wind speed - V_o (m/s)		
	0.00	30.5	42.7
160.00	58.91	58.91	62.41
200.00	60.91	59.91	62.66
250.00	60.41	58.91	61.41
315.00	58.91	58.91	60.41
400.00	61.91	58.91	60.16
500.00	62.66	58.91	59.66
630.00	63.41	60.91	60.91
800.00	65.91	62.91	62.16
1000.00	67.41	64.66	63.16
1250.00	71.91	66.91	66.41
1600.00	72.91	69.16	68.16
2000.00	73.66	70.91	70.16
2500.00	75.91	73.16	72.91
3150.00	77.66	74.91	74.91
4000.00	78.86	76.61	76.36
5000.00	80.48	78.48	78.23
6300.00	81.86	80.11	79.61
8000.00	82.41	81.16	80.66
10000.00	83.26	81.76	81.51
12500.00	83.46	81.21	83.21
16000.00	83.74	80.74	81.99
20000.00	83.46	80.96	80.96
25000.00	82.86	80.86	80.61
31500.00	82.56	80.31	79.56
40000.00	81.41	79.41	79.91
50000.00	79.76	78.26	78.76
63000.00	76.86	75.61	75.61
OASPL	93.50	91.41	91.62

JET NOISE

Out-of-Wind Microphone

Angle $\psi = 70^{o}$

$V_j = 340$ m/s $(M_j = 1.0)$

one-third octave band center frequency	1/3 octave band SPL - dB(re 2×10^{-5}Pa)		
	wind speed - V_o (m/s)		
	0.00	30.5	42.7
160.00	58.21	61.21	65.71
200.00	59.46	60.96	63.96
250.00	58.21	59.21	62.21
315.00	58.21	60.46	64.46
400.00	58.96	60.96	61.21
500.00	60.21	64.21	64.21
630.00	62.71	65.96	63.46
800.00	64.46	62.46	63.21
1000.00	66.21	64.46	64.21
1250.00	68.21	66.46	70.71
1600.00	70.21	68.46	73.21
2000.00	72.21	70.46	77.21
2500.00	74.71	72.96	77.71
3150.00	76.21	74.21	76.71
4000.00	77.66	76.16	76.91
5000.00	78.78	77.53	76.78
6300.00	80.41	79.66	78.16
8000.00	81.21	79.96	78.71
10000.00	81.81	80.31	79.81
12500.00	82.76	84.01	79.01
16000.00	81.04	80.04	78.29
20000.00	81.26	79.76	78.76
25000.00	80.16	78.41	78.41
31500.00	80.11	78.11	77.61
40000.00	79.96	78.71	78.21
50000.00	78.81	77.31	77.06
63000.00	75.16	73.41	73.66
OASPL	91.79	90.84	90.15

JET NOISE

Out-of-Wind Microphone

Angle $\psi = 80^{o}$

$V_j = 340$ m/s ($M_j = 1.0$)

one-third octave band center frequency	1/3 octave band SPL - dB(re $2x10^{-5}$Pa)		
	wind speed - V_o (m/s)		
	0.00	30.5	42.7
160.00	58.30	57.80	61.55
200.00	61.30	61.05	62.55
250.00	57.80	57.80	59.05
315.00	57.80	57.80	58.80
400.00	58.05	57.80	58.80
500.00	59.30	58.30	59.05
630.00	61.55	60.05	60.30
800.00	63.05	61.30	61.05
1000.00	65.30	62.80	63.30
1250.00	68.05	65.55	65.05
1600.00	69.80	67.55	67.05
2000.00	71.55	69.55	69.05
2500.00	73.55	71.30	71.30
3150.00	74.80	73.05	72.55
4000.00	76.20	74.20	73.70
5000.00	77.90	75.65	75.40
6300.00	79.30	77.55	77.55
8000.00	80.30	78.80	78.30
10000.00	80.05	78.05	77.80
12500.00	80.80	78.80	78.05
16000.00	79.95	77.95	77.70
20000.00	80.00	77.75	78.00
25000.00	79.05	77.05	76.80
31500.00	79.40	77.65	77.90
40000.00	77.35	75.85	75.35
50000.00	76.70	75.20	75.20
63000.00	73.65	72.65	72.40
OASPL	90.42	88.55	88.34

JET NOISE

Out-of-Wind Microphone

Angle $\psi = 90^{\circ}$

$V_j = 340$ m/s ($M_j = 1.0$)

one-third octave band center frequency	1/3 octave band SPL - dB(re 2×10^{-5}Pa)		
	wind speed - V_o (m/s)		
	0.00	30.5	42.7
160.00	58.66	57.91	61.91
200.00	61.66	60.66	62.41
250.00	57.66	57.66	58.91
315.00	57.66	57.66	59.66
400.00	57.66	57.66	58.66
500.00	58.66	57.91	58.91
630.00	60.66	59.66	60.16
800.00	62.16	60.91	60.91
1000.00	64.41	62.41	62.41
1250.00	66.41	64.66	64.16
1600.00	68.16	66.91	65.66
2000.00	70.41	68.91	68.16
2500.00	72.16	70.91	70.16
3150.00	73.66	72.41	72.16
4000.00	74.56	73.81	73.06
5000.00	76.26	75.26	74.76
6300.00	77.66	76.66	75.66
8000.00	78.66	77.66	77.41
10000.00	78.16	77.16	77.16
12500.00	78.66	79.16	77.16
16000.00	79.31	78.31	77.31
20000.00	78.61	77.86	77.11
25000.00	76.91	76.41	75.91
31500.00	78.51	77.26	77.01
40000.00	77.41	77.71	77.21
50000.00	78.81	76.06	76.81
63000.00	72.76	72.51	73.01
OASPL	89.25	88.41	87.86

<u>JET NOISE</u>

Out-of-Wind Microphone
Angle $\psi = 100^{\circ}$

$V_j = 340$ m/s ($M_j = 1.0$)

one-third octave band center frequency	1/3 octave band SPL - dB(re 2×10^{-5}Pa)		
	wind speed - V_o (m/s)		
	0.00	30.5	42.7
160.00	57.80	57.80	61.55
200.00	57.80	60.05	62.05
250.00	57.80	57.80	58.05
315.00	57.80	57.80	58.80
400.00	57.80	57.80	57.80
500.00	58.80	57.80	58.80
630.00	61.05	59.55	59.55
800.00	62.55	60.30	60.55
1000.00	64.30	62.30	61.55
1250.00	66.30	63.80	63.05
1600.00	68.30	66.55	65.55
2000.00	70.80	68.55	67.55
2500.00	72.55	70.30	69.80
3150.00	73.55	71.80	71.30
4000.00	74.95	72.95	72.45
5000.00	75.90	74.90	74.15
6300.00	77.05	75.80	75.80
8000.00	78.55	77.30	76.80
10000.00	78.80	77.55	77.55
12500.00	78.30	77.55	76.80
16000.00	78.20	77.70	76.95
20000.00	78.00	76.50	76.25
25000.00	76.80	75.30	74.80
31500.00	77.90	75.90	75.65
40000.00	77.60	76.85	76.60
50000.00	76.70	75.95	75.70
63000.00	73.65	72.40	72.15
OASPL	88.89	87.67	87.29

JET NOISE

Out-of-Wind Microphone

Angle $\psi = 110^{o}$

$V_j = 340$ m/s ($M_j = 1.0$)

one-third octave band center frequency	1/3 octave band SPL - dB(re $2x10^{-5}$Pa)		
	wind speed - V_o (m/s)		
	0.00	30.5	42.7
160.00	58.21	59.46	62.21
200.00	61.21	61.71	62.71
250.00	58.21	58.21	58.46
315.00	58.21	58.21	58.46
400.00	58.21	58.21	58.46
500.00	58.21	58.21	58.21
630.00	59.96	58.71	59.21
800.00	61.96	60.71	60.21
1000.00	64.21	62.21	61.71
1250.00	66.21	63.96	63.46
1600.00	67.96	65.71	64.46
2000.00	69.96	67.71	66.71
2500.00	71.96	69.46	68.96
3150.00	72.96	70.96	70.46
4000.00	73.61	71.86	71.11
5000.00	74.81	73.56	73.31
6300.00	76.16	74.91	74.66
8000.00	77.76	76.51	75.26
10000.00	77.66	76.16	75.91
12500.00	77.11	76.11	76.36
16000.00	77.36	75.11	75.36
20000.00	76.61	74.86	74.61
25000.00	76.36	74.36	74.86
31500.00	77.51	75.01	75.26
40000.00	75.26	73.01	73.26
50000.00	74.56	71.81	72.81
63000.00	73.26	70.76	71.51
OASPL	87.87	86.10	86.02

JET NOISE

Out-of-Wind Microphone

Angle $\psi = 115^\circ$

$V_j = 340$ m/s ($M_j = 1.0$)

one-third octave band center frequency	1/3 octave band SPL - dB(re 2×10^{-5}Pa)		
	wind speed - V_o (m/s)		
	0.00	30.5	42.7
160.00	58.50	59.00	65.00
200.00	61.25	61.50	65.00
250.00	58.50	58.50	61.00
315.00	58.50	58.50	61.00
400.00	58.50	58.50	61.00
500.00	58.50	58.50	61.00
630.00	58.50	58.50	61.00
800.00	60.50	60.25	61.00
1000.00	63.25	62.50	61.00
1250.00	65.00	63.75	62.75
1600.00	67.25	65.75	64.75
2000.00	69.00	67.00	65.75
2500.00	71.50	69.50	68.50
3150.00	72.50	71.50	70.00
4000.00	73.90	72.15	70.90
5000.00	75.35	73.10	71.60
6300.00	76.20	74.20	73.20
8000.00	77.30	75.55	74.30
10000.00	76.95	75.70	74.70
12500.00	76.40	75.90	75.15
16000.00	76.15	75.15	74.40
20000.00	75.65	74.40	73.90
25000.00	75.90	74.40	73.65
31500.00	76.55	74.55	74.05
40000.00	74.55	72.80	71.80
50000.00	72.85	71.60	70.60
63000.00	72.30	70.30	69.30
OASPL	87.25	85.78	84.77

JET NOISE

In-Wind Microphone

Angle $\psi = 20^{\circ}$

$V_j = 340$ m/s ($M_j = 1.0$)

one-third octave band center frequency	1/3 octave band SPL - dB(re 2×10^{-5} Pa)		
	wind speed - V_o (m/s)		
	0.00	30.5	42.7
160.00	57.91	81.66	99.16
200.00	59.41	80.66	100.16
250.00	61.66	79.41	97.16
315.00	64.41	79.16	91.66
400.00	67.16	79.16	92.16
500.00	70.16	77.91	88.16
630.00	73.41	77.41	87.66
800.00	76.66	77.16	83.16
1000.00	79.16	77.66	82.16
1250.00	81.91	79.41	81.91
1600.00	84.91	81.41	82.41
2000.00	87.66	83.66	83.16
2500.00	90.16	86.66	85.66
3150.00	92.16	88.66	87.66
4000.00	92.31	89.81	89.31
5000.00	93.26	90.51	90.51
6300.00	93.26	91.01	90.51
8000.00	92.81	90.56	89.81
10000.00	90.71	88.96	88.46
12500.00	88.31	87.31	87.06
16000.00	85.96	85.71	85.71
20000.00	82.66	82.91	82.66
25000.00	80.66	81.41	81.41
31500.00	80.76	81.76	81.51
40000.00	77.91	78.66	78.91
50000.00	74.51	75.51	76.01
63000.00	72.86	73.36	74.11
OASPL	101.62	99.63	105.60

JET NOISE

In-Wind Microphone

Angle $\psi = 30^{\circ}$

$V_j = 340$ m/s ($M_j = 1.0$)

one-third octave band center frequency	1/3 octave band SPL - dB(re 2×10^{-5}Pa)		
	wind speed - V_o (m/s)		
	0.00	30.5	42.7
160.00	56.52	83.52	94.77
200.00	58.27	82.52	93.77
250.00	59.52	79.77	89.77
315.00	62.02	77.52	84.77
400.00	65.02	76.77	82.77
500.00	68.27	76.02	81.52
630.00	71.27	75.52	80.77
800.00	74.02	75.27	80.02
1000.00	77.02	75.02	79.52
1250.00	79.52	76.52	79.02
1600.00	82.77	78.77	79.52
2000.00	85.77	81.02	80.52
2500.00	88.77	83.77	82.77
3150.00	91.02	86.77	85.52
4000.00	92.17	88.17	86.67
5000.00	94.12	89.62	88.62
6300.00	93.87	90.37	89.37
8000.00	93.67	90.42	89.42
10000.00	91.57	89.57	89.32
12500.00	89.92	89.17	88.67
16000.00	87.82	87.07	86.82
20000.00	85.02	84.77	84.77
25000.00	83.02	83.02	82.52
31500.00	83.37	82.87	82.62
40000.00	80.02	79.77	80.52
50000.00	77.62	77.12	77.87
63000.00	75.22	75.72	76.22
OASPL	101.97	99.34	101.45

JET NOISE

In-Wind Microphone

Angle $\psi = 40^{o}$

$V_j = 340$ m/s $(M_j = 1.0)$

one-third octave band center frequency	1/3 octave band SPL - dB(re $2x10^{-5}$Pa)		
	wind speed - V_o (m/s)		
	0.00	30.5	42.7
160.00	57.12	80.00	93.07
200.00	57.12	81.50	92.07
250.00	58.12	77.80	87.32
315.00	60.62	75.00	84.32
400.00	62.62	74.60	83.07
500.00	64.67	74.00	80.07
630.00	68.12	73.57	79.32
800.00	70.62	72.57	78.07
1000.00	73.62	72.32	77.32
1250.00	76.12	72.82	76.82
1600.00	79.12	74.32	76.32
2000.00	82.12	76.32	77.07
2500.00	84.62	78.57	77.57
3150.00	87.37	81.07	80.07
4000.00	88.02	82.72	81.22
5000.00	90.30	84.92	83.42
6300.00	91.50	85.92	84.42
8000.00	91.50	86.47	85.72
10000.00	92.30	87.37	86.12
12500.00	92.40	87.22	86.22
16000.00	90.80	86.12	85.87
20000.00	88.12	84.57	83.82
25000.00	86.80	83.82	83.57
31500.00	85.50	84.17	84.42
40000.00	82.83	81.82	82.32
50000.00	81.18	80.17	80.92
63000.00	78.02	78.02	78.27
OASPL	100.87	96.28	99.33

JET NOISE

In-Wind Microphone
Angle $\psi = 50^{\circ}$

$V_j = 340$ m/s ($M_j = 1.0$)

one-third octave band center frequency	1/3 octave band SPL - dB(re 2×10^{-5}Pa)		
	wind speed - V_o (m/s)		
	0.00	30.5	42.7
160.00	55.54	86.04	93.04
200.00	55.29	89.04	100.54
250.00	55.54	81.54	92.54
315.00	57.54	76.79	88.29
400.00	59.79	73.79	84.79
500.00	61.04	71.79	81.04
630.00	64.04	71.29	79.54
800.00	66.04	70.79	78.29
1000.00	68.29	69.79	78.04
1250.00	71.29	70.04	75.79
1600.00	73.54	71.04	74.79
2000.00	75.79	72.29	74.29
2500.00	78.54	75.04	75.04
3150.00	80.29	76.04	75.79
4000.00	81.99	78.49	77.74
5000.00	84.36	80.36	79.61
6300.00	85.49	81.49	80.74
8000.00	87.04	82.79	82.04
10000.00	87.64	84.14	83.14
12500.00	87.84	84.34	82.84
16000.00	86.12	83.37	82.37
20000.00	85.59	82.34	81.34
25000.00	84.49	81.74	80.74
31500.00	83.44	80.94	80.19
40000.00	81.54	79.54	78.79
50000.00	79.89	78.14	77.64
63000.00	77.49	76.49	76.24
OASPL	96.35	95.42	102.59

JET NOISE

In-Wind Microphone

Angle ψ = 60°

V_j = 340 m/s (M_j = 1.0)

one-third octave band center frequency	1/3 octave band SPL - dB(re 2×10^{-5}Pa)		
	wind speed - V_o (m/s)		
	0.00	30.5	42.7
160.00	54.40	76.90	85.65
200.00	53.90	78.90	90.90
250.00	54.65	78.15	89.65
315.00	56.90	74.90	84.90
400.00	58.65	72.15	81.40
500.00	60.40	71.15	77.65
630.00	62.65	70.40	77.40
800.00	65.15	69.40	76.40
1000.00	66.90	69.15	75.40
1250.00	69.40	68.90	74.65
1600.00	71.15	69.65	73.15
2000.00	73.15	71.15	73.15
2500.00	75.65	72.90	74.15
3150.00	77.15	74.65	74.65
4000.00	78.35	75.60	75.60
5000.00	80.97	78.22	77.97
6300.00	81.85	79.10	78.60
8000.00	83.15	80.65	79.90
10000.00	84.25	81.75	81.25
12500.00	84.20	81.45	80.70
16000.00	83.48	80.48	79.48
20000.00	82.45	80.70	79.95
25000.00	81.85	79.85	78.85
31500.00	81.55	79.30	78.80
40000.00	79.90	77.65	77.15
50000.00	78.75	77.00	76.00
63000.00	78.35	76.35	75.60
OASPL	93.35	91.79	96.31

JET NOISE

In-Wind Microphone

Angle $\psi = 70^{\circ}$

$V_j = 340$ m/s ($M_j = 1.0$)

one-third octave band center frequency	1/3 octave band SPL - dB(re 2×10^{-5}Pa)		
	wind speed - V_o (m/s)		
	0.00	30.5	42.7
160.00	51.78	75.03	84.53
200.00	52.53	79.53	89.03
250.00	53.03	77.78	88.03
315.00	55.03	74.03	85.28
400.00	57.28	70.53	80.53
500.00	59.03	69.53	77.78
630.00	61.53	69.53	76.53
800.00	63.78	68.78	76.28
1000.00	65.53	68.03	75.03
1250.00	68.03	68.28	74.03
1600.00	69.53	68.78	73.03
2000.00	71.78	70.28	72.28
2500.00	74.03	72.28	73.28
3150.00	75.53	73.03	73.28
4000.00	76.98	74.48	74.48
5000.00	78.10	76.60	75.85
6300.00	79.73	77.48	77.23
8000.00	80.78	78.53	78.03
10000.00	82.13	79.38	78.88
12500.00	81.83	79.08	78.33
16000.00	80.61	78.36	77.86
20000.00	80.58	78.08	78.08
25000.00	79.73	77.23	76.98
31500.00	78.93	77.18	76.68
40000.00	77.78	75.78	75.53
50000.00	77.13	75.63	75.38
63000.00	76.48	74.73	74.48
OASPL	91.15	90.10	94.92

JET NOISE

In-Wind Microphone

Angle $\psi = 80^{o}$

$V_j = 340$ m/s ($M_j = 1.0$)

one-third octave band center frequency	1/3 octave band SPL - dB(re 2×10^{-5}Pa)		
	wind speed - V_o (m/s)		
	0.00	30.5	42.7
160.00	49.58	74.83	82.08
200.00	49.83	75.08	83.58
250.00	51.08	77.08	84.33
315.00	53.33	75.33	82.33
400.00	55.83	70.33	78.33
500.00	57.58	69.58	76.33
630.00	60.33	69.58	75.58
800.00	62.33	68.08	74.83
1000.00	64.83	67.83	74.08
1250.00	67.33	67.83	73.33
1600.00	68.58	68.08	72.33
2000.00	70.83	69.08	71.83
2500.00	72.33	71.08	72.33
3150.00	74.08	72.08	72.33
4000.00	75.48	73.48	73.48
5000.00	76.93	74.93	74.68
6300.00	79.08	76.83	76.83
8000.00	80.08	78.08	77.83
10000.00	80.58	78.58	77.83
12500.00	80.58	78.33	78.08
16000.00	79.98	77.73	77.48
20000.00	79.03	77.28	76.78
25000.00	78.08	75.83	75.33
31500.00	78.68	76.68	76.43
40000.00	76.63	74.88	74.38
50000.00	76.23	74.73	74.73
63000.00	75.18	73.93	73.18
OASPL	90.04	89.18	92.22

JET NOISE

In-Wind Microphone

Angle $\psi = 90^o$

$V_j = 340$ m/s ($M_j = 1.0$)

one-third octave band center frequency	1/3 octave band SPL - dB (re $2x10^{-5}$Pa)		
	wind speed - V_o (m/s)		
	0.00	30.5	42.7
160.00	48.50	72.50	81.50
200.00	48.25	71.25	79.75
250.00	49.00	71.50	81.25
315.00	51.50	71.25	79.75
400.00	54.50	70.50	78.25
500.00	56.25	69.25	77.50
630.00	58.50	69.00	76.50
800.00	61.00	68.25	76.25
1000.00	63.25	67.25	74.75
1250.00	65.00	67.50	74.25
1600.00	67.25	67.00	72.50
2000.00	69.25	68.50	72.25
2500.00	71.25	70.25	72.25
3150.00	72.25	71.75	72.00
4000.00	73.90	72.90	73.15
5000.00	75.85	74.35	74.35
6300.00	77.00	75.75	75.50
8000.00	78.75	77.25	76.75
10000.00	79.00	77.50	77.00
12500.00	79.75	78.00	77.50
16000.00	78.40	76.90	76.65
20000.00	77.70	76.45	75.95
25000.00	75.75	75.00	75.00
31500.00	77.10	76.35	75.85
40000.00	74.80	74.55	73.80
50000.00	74.90	74.40	73.90
63000.00	74.85	73.85	73.10
OASPL	88.59	88.10	91.00

JET NOISE

In-Wind Microphone

Angle $\psi = 100^{o}$

$V_j = 340$ m/s $(M_j = 1.0)$

one-third octave band center frequency	1/3 octave band SPL - dB(re $2x10^{-5}$Pa)		
	wind speed - V_o (m/s)		
	0.00	30.5	42.7
160.00	47.69	72.69	81.44
200.00	47.69	72.69	81.44
250.00	47.44	71.94	79.44
315.00	50.44	71.44	78.44
400.00	53.69	70.69	78.19
500.00	55.44	69.44	76.44
630.00	56.94	69.19	75.94
800.00	59.94	68.19	74.44
1000.00	61.94	67.19	73.94
1250.00	64.44	66.94	72.94
1600.00	66.44	66.69	71.44
2000.00	68.94	67.44	70.69
2500.00	70.69	69.19	70.94
3150.00	71.94	70.19	71.19
4000.00	73.84	71.84	71.84
5000.00	74.79	73.54	73.04
6300.00	76.69	74.94	74.69
8000.00	77.94	76.19	75.94
10000.00	78.69	76.44	76.44
12500.00	78.44	76.94	76.94
16000.00	77.84	76.59	76.09
20000.00	76.89	75.64	74.89
25000.00	75.94	74.69	74.44
31500.00	76.79	75.04	75.04
40000.00	74.49	73.49	73.74
50000.00	75.09	73.84	73.59
63000.00	74.04	73.29	73.04
OASPL	88.03	87.46	90.43

JET NOISE

In-Wind Microphone

Angle $\psi = 110^o$

$V_j = 340$ m/s $(M_j = 1.0)$

one-third octave band center frequency	1/3 octave band SPL - dB(re $2x10^{-5}$Pa)		
	wind speed - V_o (m/s)		
	0.00	30.5	42.7
160.00	47.30	72.80	82.80
200.00	47.55	72.80	82.55
250.00	46.80	72.80	79.80
315.00	48.55	71.55	79.80
400.00	51.80	71.05	78.55
500.00	55.80	70.30	77.05
630.00	57.05	70.05	76.30
800.00	58.55	68.30	74.80
1000.00	61.80	67.30	73.55
1250.00	63.55	66.80	73.30
1600.00	65.55	66.55	71.30
2000.00	67.55	66.80	71.30
2500.00	69.80	68.80	70.80
3150.00	71.05	69.30	70.80
4000.00	72.20	70.95	70.95
5000.00	73.90	72.40	72.40
6300.00	75.50	74.00	73.50
8000.00	77.10	75.35	75.35
10000.00	77.50	76.00	75.25
12500.00	77.45	75.70	75.70
16000.00	76.20	74.20	74.45
20000.00	74.95	73.95	73.95
25000.00	75.20	74.20	73.95
31500.00	76.10	74.85	74.60
40000.00	74.35	73.35	73.10
50000.00	73.40	71.90	72.15
63000.00	72.85	71.85	71.35
OASPL	86.92	86.76	90.67

JET NOISE

In-Wind Microphone

Angle ψ = 115^o

V_j = 340 m/s (M_j = 1.0)

one-third octave band center frequency	1/3 octave band SPL - dB(re $2x10^{-5}$Pa)		
	wind speed - V_o (m/s)		
	0.00	30.5	42.7
160.00	47.73	71.48	79.73
200.00	47.23	71.23	79.98
250.00	46.98	70.98	79.73
315.00	48.73	70.48	79.48
400.00	50.98	69.98	77.98
500.00	55.23	69.23	76.48
630.00	57.23	68.73	75.98
800.00	58.23	67.73	75.23
1000.00	59.98	66.48	73.98
1250.00	63.23	66.23	73.48
1600.00	64.73	65.48	71.23
2000.00	66.98	66.23	70.98
2500.00	69.23	67.98	70.48
3150.00	70.48	69.23	70.23
4000.00	72.13	70.63	70.88
5000.00	73.83	72.33	72.33
6300.00	74.68	73.68	72.93
8000.00	76.53	75.53	75.03
10000.00	76.93	75.43	75.18
12500.00	77.63	75.63	75.88
16000.00	75.88	74.88	74.63
20000.00	75.13	73.63	73.63
25000.00	75.13	73.88	74.38
31500.00	75.78	74.78	74.53
40000.00	74.03	72.78	73.03
50000.00	73.08	71.58	71.33
63000.00	72.53	71.28	70.78
OASPL	86.63	86.32	89.81

REFERENCES

1. Packman, A.B.; Ng, K.W.; and Paterson, R.W.: Effect of Simulated Forward Flight on Subsonic Jet Exhaust Noise. AIAA Paper No. 75-869, June, 1975.

2. Beulke, M.R.; Clapper, W.S.; McCann, E.O.; and Morozumi, H.M.: A Forward Speed Effects Study on Jet Noise from Several Suppressor Nozzles in the NASA/Ames 40- by 80- Foot Wind Tunnel. NASA CR-114741, 1974.

3. Strout, Frank G.: Flight Effects on Noise Generated by the JT8D-17 Engine in a Quiet Nacelle and a Conventional Nacelle as Measured in the NASA Ames 40- by 80-Foot Wind Tunnel. Report to NASA Ames Research Center under Contract No. NAS 2-8213, 1975.

4. Cocking, B.J.; and Bryce, W.D.: Subsonic Jet Noise in Flight Based on Some Recent Wind Tunnel Tests. AIAA Paper No. 75-462, March, 1975.

5. DeBelleval, J.; Chen, C.Y.; and Perulli, M.: Investigation of Inflight Noise Based on Measurements in an Anechoic Wind Tunnel. Paper presented at the Sixth International Congress on Instrumentation and Aerospace Simulation Facilities, Ottawa, Canada, September, 1975.

6. Plumblee, H.E., Jr., ed.: A Study of the Effects of Forward Velocity on Turbulent Jet Mixing Noise. Report to NASA Lewis Research Center under Contract No. NAS3-18540, 1975.

7. Kadman, Y.; and Hayden, R.E.: Design and Performance of High-Speed Free-Jet Acoustic Wind Tunnel. AIAA Paper No. 75-531, March, 1975.

8. Ffowcs Williams, J.E.: The Noise from Turbulence Convected at High Speed. Phil. Trans. Royal Society, A255, 1963, pp. 469-502.

9. Sarohia, V. and Massier, P.F.: Important Flow Field Effects on Jet Noise Under Flight Conditions. Paper presented at the Workshop on Effects of Forward Velocity on Jet Noise, NASA Langley Research Center, January, 1976.

10. Ribner, H.S.: The Generation of Sound by Turbulent Jets. Advances in Applied Mechanics, Vol. 8, Academic Press, Inc., 1964, pp. 104-178.

11. Mani, R.: The Influence of Jet Flow on Jet Noise, Part I, The Noise of Unheated Jets. J. Fluid Mech., 73, 1976, pp. 753-778.

12. Tester, B.J.; and Morfey, C.L.: Developments in Jet Noise Modeling - The Theoretical Predictions and Comparisons with Measured Data. J. Sound and Vib., 46, pp. 79-103.

13. Morse, P.M.; and Ingard, U.: Theoretical Acoustics. McGraw-Hill Book Co., Inc., 1968, pp. 699-700.

14. Cole, J.E.; and Sarris, I.I.: Theoretical Results Pertinent to Measurements of Jet Noise in Wind Tunnels. Proceedings of the Third Interagency Symposium on University Research on Transportation Noise, University of Utah, pp. 467-474, 1975.

15. Ahuja, K.K.; and Bushell, K.W.: An Experimental Study of Subsonic Jet Noise and Comparison with Theory. J. Sound Vib., 30, 1973, pp. 317-341.

16. Rudd, M.J.: A Note on the Scattering of Sound in Jets and the Wind. J. Sound Vib., 26, 1973, pp. 551-560.

17. Candel, S.; Guedel, A.; and Julienne, A.: Refraction and Scattering of Sound in an Open Wind Tunnel Flow. Paper presented at the Sixth International Congress on Instrumentation and Aerospace Simulation Facilities, Ottawa , Canada, 1975.

18. Amiet, R.K.: Correction of Open Jet Wind Tunnel Measurements for Shear Layer Refraction. AIAA Paper No. 75-532, March, 1975.

19. Tester, B.J.; and Burrin, R.H.: On Sound Radiation from Sources in Parallel Sheared Jet Flows, From the Generation and Radiation of Supersonic Jet Noise. Lockheed-Georgia Company Report LG75ER0010, 1974, pp. 1-28 to 1-56.

20. Shubert, L.K.: Numerical Study of Sound Refraction by a Jet Flow, Part II: Wave Acoustics. J. Acoust. Soc. Amer., 51, 1972, pp. 447-463.

21. Anon: Proposed Format for Revising Aerospace Information Report No. 876. Society of Automotive Engineers.

22. Stone, J.R.: Interim Prediction Method for Jet Noise. NASA TM X-71618.

23. Anon: Instructions and Applications for Brüel and Kjaer Microphone Cartidges Type 4135/36. Brüel and Kjaer, Copenhagen, Denmark, May, 1963.

24. Anon: Frequency Response of the Model 4136 1/4" Microphone with Old and New Nose Cones. Brüel and Kjaer, Cleveland, Ohio, October, 1975.